Vol. 680: 137–161, 2021
https://doi.org/10.3354/meps13906

MARINE ECOLOGY PROGRESS SERIES
Mar Ecol Prog Ser

Published December 9

Contribution to the Theme Section 'Advancing dynamic modelling of marine populations and ecosystems'

Simulating fish population responses to elevated CO_2: a case study using winter flounder

Klaus B. Huebert[1,*], Kenneth A. Rose[1], R. Christopher Chambers[2]

[1]Horn Point Laboratory, University of Maryland Center for Environmental Science, Cambridge, Maryland 21613, USA
[2]Howard Marine Sciences Laboratory, Northeast Fisheries Science Center, NOAA Fisheries Service, Highlands, New Jersey 07732, USA

ABSTRACT: Scaling experimentally derived effects of CO_2 on marine fauna to population responses is critical for informing management about potential ecological ramifications of ocean acidification. We used an individual-based model of winter flounder to extrapolate laboratory-derived effects of elevated CO_2 assumed for early life stages of fish to long-term population dynamics. An offspring module with detailed hourly to daily representations of spawning, growth, and mortality that incorporates potential elevated CO_2 effects was linked to an annual time-step parent module. We calibrated the model using a 40 yr Reference simulation (1977–2016) that included gradual warming and then performed 'Retrospective' simulations that assumed a suite of elevated CO_2 effects by changing fertilization rate, mortality rate of embryos due to developmental malformations, larval growth rate, and size-at-settlement. 'Recovery' simulations that started at low population size were then used to further explore possible interactions between the effects of CO_2 and warming on population productivity. Warming had a major negative effect on the simulated winter flounder population abundance, and reduced larval growth had the largest single impact among the CO_2 effects tested. When a combination of the assumed CO_2 effects was imposed together, average annual recruitment and spawning stock biomass were reduced by half. In the Recovery simulations, inclusion of CO_2 effects amplified the progressive decrease in population productivity with warming. Our analysis is speculative and a first step towards addressing the need for extrapolating from laboratory effects of ocean acidification to broader, ecologically relevant scales.

KEY WORDS: Elevated CO_2 · Fish · Model · Ocean acidification · Population · Winter flounder

1. INTRODUCTION

Absorption of anthropogenic CO_2 is projected to increase the acidification of ocean and coastal marine waters (Hartin et al. 2016). The physiological and ecological effects of elevated CO_2 concentrations on early life stages of fish have been studied in laboratory experiments using a variety of taxa (Munday et al. 2010, Clements & Hunt 2015). The laboratory results for fish and other taxa have been mixed, with effects ranging from negative to none to positive (Harvey et al. 2013, Cattano et al. 2018) depending on study species, response variables examined, and CO_2 treatment concentrations used in the experiments.

Extrapolation of experimentally derived effects of CO_2, and ocean acidification (OA) in general, to population-level responses in nature is difficult but important (Pankhurst & Munday 2011, Queirós et al. 2015, Nagelkerken & Munday 2016). As is the case for biological effects studies of contaminants (Suter 2016), laboratory-based CO_2 effects studies have provided valuable information describing how groups of individuals are affected under controlled conditions. Such data (e.g. larval growth rate) can be

*Corresponding author: khuebert@umces.edu

Publisher: Inter-Research · www.int-res.com

used to identify CO_2 concentrations that might lead to significant consequences in nature. However, the appropriate scale for determining ecological relevance and the scale at which management operates are broader and at higher levels of biological organization (e.g. population, food web). What is needed is a set of tools for moving laboratory-demonstrated effects closer to the ecologically relevant endpoints that align with the scale of resource management (Rose et al. 2003, Townsend et al. 2019).

There are many challenges involved with scaling effects on individuals up to higher levels for understanding consequences to living marine resources (Rose 2000). Populations of fish and many other marine taxa exhibit complex life cycles that involve life stages which often use distinct habitats and whose vital rates (growth, mortality, reproduction) are influenced by multiple and often interacting environmental factors (Petitgas et al. 2013, Archambault et al. 2018). Further, population responses often lag in time due to the complex ways that effects propagate through the life cycle (Rose 2000, Ottersen et al. 2010, Pasquaud et al. 2013). Population responses are also influenced by indirect effects, which may be mediated by other components of the food web and environmental variables that may themselves be affected by the same or other stressors (Sswat et al. 2018, Bartley et al. 2019). Analysis of time-series data can provide useful information about climate and other environmental effects on such populations (e.g. Morrongiello et al. 2014, Rogers & Dougherty 2019), but the annual frequency of many of our resource surveys and catch data limit the robustness of statistical approaches focused on correlation (Myers 1998, Gargett et al. 2001). One limitation of time-series analysis is the risk associated with extrapolating beyond the range of environmental conditions observed in the time series.

Simulation modeling is an additional tool that complements laboratory and statistical approaches for tracking the effects of multiple factors through complex life cycles. Simulation models may be particularly useful for predicting effects of elevated CO_2 due to CO_2 affecting multiple processes (growth, mortality, development) across multiple life stages. Here, we employed an individual-based simulation modeling approach to scale up from laboratory-documented effects of CO_2 on fish early life stages to long-term population dynamics. We used an individual-based model (IBM) to capture detailed ecological processes of the early life stages to enable representation of some of the dominant experimentally revealed CO_2 effects. The IBM builds on a prior winter flounder IBM (Chambers et al. 1995, Rose et al. 1996) and a generic larval fish IBM (Huebert & Peck 2014). An early life stage (offspring) module was linked to a parent module to achieve multigenerational simulations and the extrapolation of early life stage CO_2 effects to long-term population responses. We chose winter flounder *Pseudopleuronectes americanus* as our focal species due to its historic importance in NE USA, its use in prior CO_2 laboratory experiments, and its historically declining populations related to regional warming. Our analysis demonstrates how laboratory information can be scaled up to long-term population dynamics under changing environmental conditions. With some loss of generality, we based the IBM on winter flounder information in order to allow for comparisons to field data, thereby ensuring sufficient realism of the underlying population dynamics. The simulated effects of CO_2 are not sufficiently based on species-specific information to allow interpretation of results as likely winter flounder responses. Thus, the elevated CO_2 simulations demonstrate the types of information needed from future studies and illustrate the possible population-level responses of fish when reasonable elevated CO_2 effects are coupled to a realistic underlying population dynamics model.

2. METHODS

2.1. Overview

We coupled a detailed IBM for the early life stages (offspring module) with a coarser IBM for age-class 1 through adults (parent module). The parent module explicitly follows females; when totals (males and females) were needed (e.g. to compare parent module biomass to adult biomass reported in field data), we assumed a 1:1 sex ratio. Typical ratios (females to males) for winter flounder range from 1:1 to favoring females (≤3:1) (Klein-MacPhee 1978, Danila 2000); assuming a ratio other than 1:1 would be accommodated in calibration and generate similar results. The offspring module tracks offspring of each parent individual in terms of daily development and survival through early ontogeny (oocytes, ova, embryos, and yolk-sac larvae) and then in terms of hourly growth (bioenergetics) and daily survival through the remainder of the first year of life (i.e. feeding larvae and young-of-the-year [YOY] juveniles). The surviving juveniles then enter the parent module as age-1 and are tracked until 15 yr of age. The parent module updates length and survival of each individual annually and determines

reproduction in the next year's offspring module, thereby closing the life cycle.

The physical environment was modeled as a single well-mixed spatial box characterized by daily water temperature and day length (daily fraction of daylight) representative of winter flounder habitat in the southern portion of their range (Chambers et al. 1995). We used the temperature data (Fig. 1) monitored during 1976–2016 at the Niantic River, Rhode Island, USA (Millstone Environmental Laboratory 2017), where the winter flounder has been studied for multiple decades (Danila 2000, Lorda et al. 2000). Day length was estimated using the NOAA solar calculator (R package 'maptools'; Bivand & Lewin-Koh 2021) for a latitude of 41.3° N (Niantic Bay, Connecticut). A suite of assumed CO_2 effects were imposed as changes to egg fertilization rate, mortality at hatching, growth rate of feeding larvae, and size-at-settlement. While these changes were based on laboratory experiments on winter flounder and other species, their magnitudes, and even directions in some cases, are not well established. Consequently, model simulation results of responses to elevated CO_2 should be viewed as speculative and not specific to winter flounder.

The winter flounder IBM is described in general terms below; the rationales, supporting information for the formulations, and estimation of parameter values are provided in Supplements 1–3 at www.int-res.com/articles/suppl/m680p137_supp.pdf (for all supplements). Further details are provided on the overall flow of model calculations (Fig. 2) and model parameters (Tables 1 & 2). The IBM uses an approach where a fixed number of model super-individuals is followed throughout the simulation (Scheffer et al. 1995, Rose et al. 2015). Each super-individual represents a variable number or 'worth' of individuals that is reduced over time by mortality. All outputs are expressed in terms of worth-adjusted values to reflect population-level dynamics. Both modeling and data analysis were performed using R versions 3.3 to 4.0 (R Development Core Team 2016).

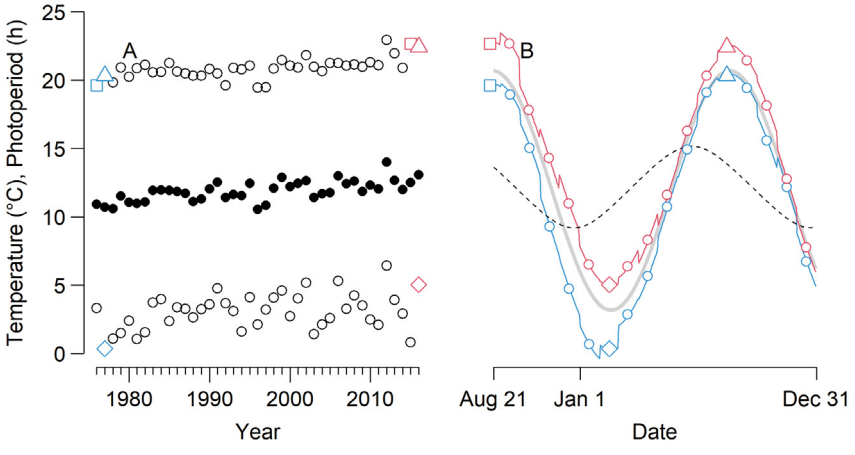

Fig. 1. Environmental input data for the individual-based model (IBM) of winter flounder. (A) Coldest and warmest monthly mean temperature (open symbols, months with colored symbols also shown in panel B for each year and the associated annual mean temperature (solid circles). (B) Daily photoperiod (dashed, not dependent on year) and temperature (solid) affecting the first (blue; 1977) and last (red; 2016) year-classes (recruitment) in the Reference simulations. Daily temperature was calculated from a time series of monthly mean temperature by fitting a sinusoidal curve (gray) to all data and shifting segments of this curve, one month at a time, to match specific monthly mean temperatures (symbols). Both panels show the gradual warming during the 1977–2016 time period

2.2. Offspring module

The offspring module tracks individuals through 6 sequential ontogenetic stages: oocytes within the adult (used to determine onset of spawning); ova within the adult (until their release into the environment and fertilization); embryos (from fertilization of ova until hatching); yolk-sac larvae (hatching to first feeding); feeding larvae (first feeding until settlement to juveniles); and YOY juveniles (juveniles until the end of the calendar year). Oocytes and ova are within the adult females. The oocyte stage is only used to calculate the onset of the ova stage in any given year; the ova stage is when the number of gametes produced by females in the parent module is determined and then used to initialize new super-individuals that are added to the offspring module. Juvenile individuals at the end of the calendar year (31 December) are considered recruits.

2.2.1. Offspring development

The offspring module starts on January 1 of each year, receives new ova super-individuals from the parent module (1 per adult female super-individual) at the onset of spawning (January–March) and ends on 31 December. The day of spawning onset is determined by tracking cumulative oocyte development of all parent super-individuals from 0–100%. A random value of required ova development be-

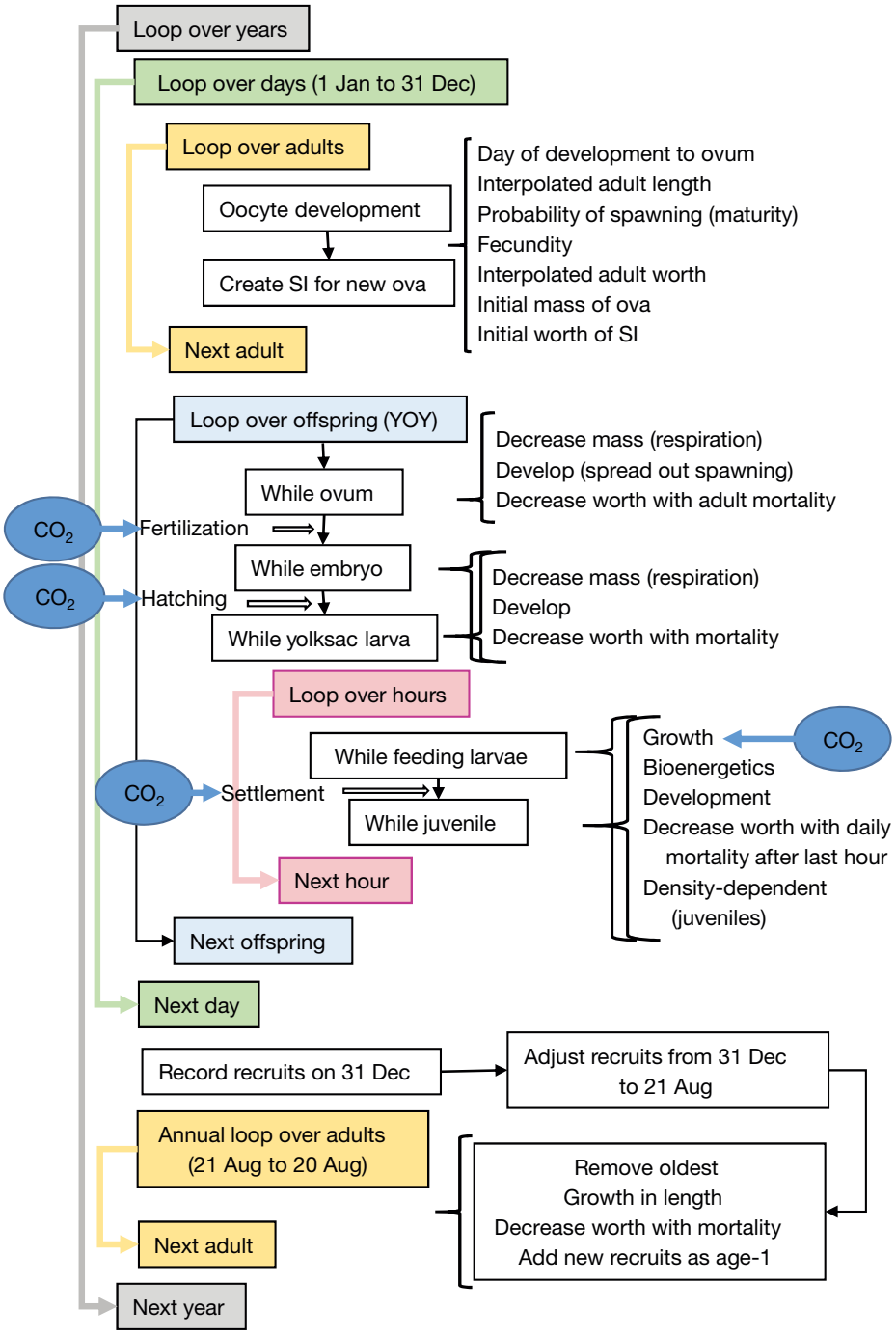

Fig. 2. Flow of calculations for the offspring and parent modules of the IBM. The assumed effects of elevated CO_2 included in model simulations are shown as blue ovals: decreased (or increased) fertilization, mortality at hatching due to developmental malformations, smaller size-at-settlement, and slower (or faster) growth rate of larvae. SI: super-individuals

fore spawning, drawn from a triangular distribution (0–100%, mode of 50%), is assigned to each individual. Varying the duration of the ova stage in the simulations creates a distribution of times during the spawning season when eggs are released into the environment.

In all stages prior to feeding larvae (oocytes, ova, embryos, and yolk-sac larvae), stage development (S) is represented as a daily (Δt = 24 h) accumulation of fractional increments of development (ΔS) that depend on development rate (a_s) adjusted for the effects of temperature (T) using a Q_{10} effect (Q_s):

Table 1. Model parameters, descriptions, units, values (Reference simulation), and sources for the YOY life stages in the offspring module. (t): tuned values determined by adjustment during calibration (see Supplements 2 & 4); C: consumption; G: gut content; L: total length; M: dry mass; R: respiration rate; T: temperature; z: mortality rate; σ: density-dependent mortality. Sources: [1] Williams (1975); [2] Buckley et al. (1990); [3] McElroy et al. (2013); [4] McBride et al. (2013); [5] Buckley et al. (1991); [6] R. C. Chambers unpubl. data; [7] Cetta & Capuzzo (1982); [8] Rogers (1976); [9] Huebert & Peck (2014); [10] Frame (1973a); [11] Laurence (1975); [12] Voyer & Morrison (1971); [13] Huebner & Langton (1982); [14] Laurence (1977); [15] Worobec (1984); [16] Klein-MacPhee (1978); [17] Frame (1973b); [18] Thornton & Lessem (1978); [19] Buckley (1981); [20] DeLong et al. (2001); [21] Houde & Zastrow (1993); [22] Keller & Klein-MacPhee (2000); [23] Millstone Environmental Laboratory (2017); [24] Pearcy (1962)

Symbol	Description	Units	Oocyte	Ova	Embryos	Yolk-sac larvae	Feeding larvae	Juveniles
a_s	Development rate (10°C)	d^{-1}	0.005 (t)	≥0.02[a] (t)	0.1280 [1]	0.2238 [2]		
Q_s	T scaling of development		1.6 (t)	1.6 (t)	4.85 [1]	3.2 [2]		
a_f	Fecundity (1 mm)			0.004654 [3]				
b_f	L scaling of fecundity			3.28 [3]				
a_p	Minimum L_{parent} at maturity	mm		200 [4]				
b_p	Maximum L_{parent} at maturity	mm		390 [4]				
c_p	Modal L_{parent} at maturity	mm		291 [4]				
a_0	Intercept of initial M	µg		19.97 [5]				
b_0	L scaling of initial M	µg mm^{-1}		0.09784 [5]				
a_v	Fertilization success (0°C)			0.8663[c] [5]				
b_v	T scaling of fertilization	$°C^{-1}$		−0.01308[c] [6]				
γ	M retained at hatch				0.49 [7]			
a_h	Hatching survival (0°C)				0.8314[c] [8]			
b_h	T scaling of hatching	$°C^{-1}$			−0.02567[c] [8]			
α	Foraging activity						0.01823 (t)	2.3593 (t)
β	Digestive efficiency						0.675[c] [9]	0.675 [9]
a_r	R/M (10°C)	d^{-1}		0.005545[b] [5]	0.02583[b] [7]	0.05658[b] [7]		
a_r	R/M (1 mm, 10°C)	h^{-1}					0.02168 [7, 10–12]	0.02168 [7, 10–12]
b_r	L scaling of R/M						−0.9621 [7, 10–12]	−0.9621 [7, 10–12]
Q_r	T scaling of R/M			2.781 [7, 10–12]	2.781 [7, 10–12]	2.781 [7, 10–12]	2.781 [7, 10–12]	2.781 [7, 10–12]
a_d	Gut evacuation rate (1 mm, 10°C)	h^{-1}					0.2296 [13–14]	0.2296 [13–14]
b_d	L scaling of a_d						−0.1415 [13–14]	−0.1415 [13–14]
Q_d	T scaling of a_d						2.5 [9, 15]	2.5 [9, 15]
a_g	G/M limit (1 mm)						0.4136 [13–14]	0.4136 [13–14]
b_g	L scaling of G/M						−0.5786 [13–14]	−0.5786 [13–14]
a_c	C/M (1 mm, 10°C)	h^{-1}					0.7668(t)	0.7668 (t)
b_c	L scaling of C/M						−1.233 (t)	−1.233 (t)
t1	T strongly affected by cold	°C					0 [16]	0 [16]
t2	T barely affected by cold	°C					14 [17]	14 [17]
t3	T barely affected by heat	°C					18 [17]	18 [17]
t4	T strongly affected by heat	°C					30 [16]	30 [16]
k1	T effect at $t1$						0.05622 (t)	0.05622 (t)
k2	T effect at $t2$						0.98 [18]	0.98 [18]
k3	T effect at $t3$						0.98 [18]	0.98 [18]
k4	T effect at $t4$						0.2924 (t)	0.2924 (t)
a_b	M (1 mm)	µg					0.3161 [10, 19]	0.3161 [10, 19]
b_b	L scaling of M						3.371 [10, 19]	3.371 [10, 19]
a_m	z (1 mm, 10°C)	d^{-1}			0.5916 (t)	0.5916 (t)	0.5916 (t)	0.5916 (t)
b_m	L scaling of z				−1 [20–24]	−1 [20–24]	−1 [20–24]	−1 [20–24]
d_m	Scaling of σ							3.877e−12 (t)
Q_m	T scaling of z				2 [21]	2 [21]	2 [21]	2 [21]

[a] r^{-1}, with r randomly drawn from a triangular distribution of minimum 0, mode 25, and maximum 50
[b] Estimated by decrease in dry mass
[c] Except for CO_2 effects (slower growth: β = 0.65; faster growth: β = 0.70; increased fertilization: a_v = 0.9552, b_v = −0.006240, decreased fertilization: a_v = 0.8007, b_v = −0.01571, malformed: a_h = 0.6236, b_h = 0.1925)

Table 2. Model parameters, description, value (Reference simulation), and source for growth and mortality in the parent module. Sources: [1] Witherell & Burnett (1993); [2] NEFSC (2011)

Symbol	Description	Units	Value	Source
L_∞	Maximum length	mm	490	[1]
k_v	Brody growth coefficient		0.31	[1]
A_v	Age at $L = 0$	yr	0.25	[1]
m_n	Natural mortality rate		0.3	[2]
m_f	Fishing mortality rate		0.29	[2][a]
i	Rate of m_f increase		0.03237	[1, 2]
$L_{50\%}$	Length at 50% m_f	mm	247.3	[1, 2]

[a]Estimate for maximum sustainable yield

$$\frac{\Delta S}{\Delta t} = a_s \cdot Q_s^{\frac{T-10}{10}} \quad (1)$$

The transition from one stage to the next occurs at the end of the day when the sum of the daily fractional increments exceeds 1.0.

The offspring super-individuals are initiated at the onset of the ova stage. The initial worth (N_{ova}) of each ova-stage super-individual (one for each female parent) is the product of the worth of the parent interpolated to the date when ova are initiated (N_{parent}; see Eq. 19 for parent module mortality), the probability of the parent spawning (P), and the annual fecundity (F) of the parent:

$$N_{ova} = N_{parent} \cdot P \cdot F \quad (2)$$

Annual fecundity is calculated from the length of the parent interpolated to the date when ova are initiated (L_{parent}; see Eq. 18 for parent module growth; with coefficient a_f and exponent b_f):

$$F = a_f \cdot (L_{parent})^{b_f} \quad (3)$$

P increases with L_{parent}, assuming a triangular distribution of length at sexual maturity (with minimum a_p, maximum b_p, and mode c_p). Initial mass of the super-individual (M_{ova}; µg dry mass) is a linear function of L_{parent} (with intercept a_0 and slope b_0):

$$M_{ova} = a_0 + b_0 \cdot L_{parent} \quad (4)$$

At the end of the ova stage, ova are released from the female and may become fertilized embryos. Fertilization success is modeled as a linear function of temperature (with intercept a_v and slope b_v) and determines the fraction of super-individual worth carried over from the ova stage to the embryo stage (N_{embryo}):

$$N_{embryo} = N_{ova} \cdot (a_v + b_v \cdot T) \quad (5)$$

The embryonic period ends at hatching into yolk-sac larvae. An adjustment to yolk-sac larvae mass (M_{ysl}) is applied at hatching to account for tissues shed at hatching (Cetta & Capuzzo 1982), with a retained fraction of tissues (γ):

$$M_{ysl} = M_{embryo} \cdot \gamma \quad (6)$$

Hatching survival is a linear function of the temperature on the day of hatching (with intercept a_h and slope b_h):

$$N_{ysl} = N_{embryo} \cdot (a_h + b_h \cdot T) \quad (7)$$

Embryos and yolk-sac larvae have a constant length (L; mm total length) of 4 mm, which is only used to calculate their mortality rate. When yolk-sac larvae develop into feeding larvae, their development switches from purely temperature-dependent to bioenergetics-based growth. Increases in the length of feeding larvae and juveniles are computed from mass according to an allometric relationship in body shape ($M = a_b \cdot L^{b_b}$). Feeding larvae metamorphose into juveniles and settle when they reach a length of 8 mm.

2.2.2. Respiration and growth

Each day, the mass of ova, embryos, and yolk-sac larvae is decremented based on their respiration rate ($\Delta M/\Delta t = -R$; µg d^{-1}), which is expressed as a proportion of mass (a_r) and is related to temperature (with Q_{10} parameter Q_r):

$$R = M \cdot a_r \cdot Q_r^{\frac{T-10}{10}} \quad (8)$$

Growth in mass of feeding larvae and juveniles uses bioenergetics in hourly ($\Delta t = 1$ h) time steps. Dry mass is lost to routine respiration and foraging activity (α), and mass is gained via digestion (D; µg h^{-1}) with a conversion efficiency (β):

$$\frac{\Delta M}{\Delta t} = -R \cdot (1 + \alpha) + D \cdot \beta \quad (9)$$

Routine respiration depends on fish length (with coefficient a_r and exponent b_r) and temperature (with Q_{10} parameter Q_r):

$$R = M \cdot a_r \cdot L^{b_r} \cdot Q_r^{\frac{T-10}{10}} \quad (10)$$

Digestion, which depends on length (with coefficient a_d and exponent b_d) and temperature (with Q_{10} parameter Q_d), is a fraction of gut content (G; µg) carried over from previous time steps:

$$D = G \cdot a_d \cdot L^{b_d} \cdot Q_d^{\frac{T-10}{10}} \quad (11)$$

Gut content is tracked every hour by removal of digestion and the addition of new consumption (C; µg h^{-1}), up to a limit ($\hat{G}$; µg):

$$\frac{\Delta G}{\Delta t} = \min\left(-D + C, \hat{G} - G\right) \quad (12)$$

The gut content limit represents satiation and is a function of length (with coefficient a_g and exponent b_g):

$$\hat{G} = M \cdot a_g \cdot L^{bg} \quad (13)$$

Consumption is a fraction of mass calculated from the daylight fraction (λ) of the time step (e.g. 0.5 if sunset occurs halfway through the time step) and depends on length (with coefficient a_c and exponent b_c) and a flexible temperature-effect function $f(T)$:

$$C = \lambda \cdot M \cdot a_c \cdot L^{b_c} \cdot f(T) \quad (14)$$

If the value of consumption computed from length and temperature exceeds the amount that leads to satiation, then the excess amount is not added to gut content (Eq. 12). The temperature-effect function for consumption was proposed by Thornton & Lessem (1978) and is widely used in bioenergetics modeling (e.g. Deslauriers et al. 2017). The function is a smooth curve defined by 4 matched values of temperature ($t1$, $t2$, $t3$, and $t4$) and associated function values ($k1$, $k2$, $k3$, $k4$). In our use of the function for feeding larvae and juveniles, $f(T)$ rises rapidly from a value of 0.056 at 0°C to a value of 0.98 at 14°C, stays between 0.98 and 1.00 until 18°C, and then declines above 18°C to 0.29 at 30°C (Table 1).

2.2.3. Mortality

The worth (N) of each super-individual (ova through adults) is decreased daily to account for mortality (in addition to mortality of unfertilized ova and embryos that fail to hatch). The natural and fishing mortality of adults (Eq. 19 with Δt = 24 h) is used for ova because they are within the female. Embryos through juveniles are subjected to a mortality rate (z), with an additional density-dependent mortality for juveniles, which is expressed as a survival fraction (σ):

$$\Delta N = N \cdot e^{-z_t \cdot \Delta t} \cdot \sigma - N \quad (15)$$

Mortality rate is a function of length (with coefficient a_m and exponent b_m) and temperature (with Q_{10} parameter Q_m):

$$z = a_m \cdot L^{b_m} \cdot Q_m^{\frac{T-10}{10}} \quad (16)$$

Density-dependent mortality is imposed for the space-limited benthic juvenile stage (Myers & Cadigan 1993, van der Veer et al. 2000, DeLong et al. 2001), and survival is a decreasing function of total YOY juvenile abundance (summed worths; with coefficient d_m):

$$\sigma = \begin{cases} \left(1 + d_m \cdot \sum N_{\text{juvenile}}\right)^{-1} & \text{for juveniles} \\ 1 & \text{otherwise} \end{cases} \quad (17)$$

The value of σ for juveniles is nearly 1 at very low abundances and decreases to approximately 0.9 at high abundances. Daily mortality is applied after the last hour of each day for the feeding larvae and juveniles. The compounding effect of σ over many days has a strong influence on the annual survival fraction of juveniles.

2.2.4. Recruitment of offspring

Super-individuals in the offspring module are followed from their initiation as ova until 31 December (about 9 mo from hatching). Recruitment is defined here as the number of surviving juveniles. A representative sub-sample (see Supplement 1) of super-individuals is taken on 31 December and they are entered into the parent module. The sub-sampling step balances the number of parent super-individuals lost at the end of their lifespan with the number gained from recruitment, and thus enables a fixed number of model super-individuals to be followed throughout the simulation. To account for the period from their exit from the offspring module to when they enter and synchronize with the annual cycle of the parent module (i.e. 31 December to 21 August), we apply a partial year (232 d) of growth and natural mortality to the recruits.

2.3. Parent module — closing the life cycle

The parent module tracks super-individuals that enter each year on an annual basis (21 August to August 20, the estimated onset of oocyte development; see Supplement 2) until their eventual removal at a maximum age (lifespan) of 15 yr. Each year, the super-individuals of the terminal age class are removed and replaced by super-individuals representing the recruitment of a new year-class cohort from the offspring module. Growth in length (L; mm total length) of parent super-individuals follows a von Bertalanffy age-length relationship:

$$L = L_\infty \cdot \left(1 - e^{-k_v \cdot (A - A_v)}\right) \quad (18)$$

Age (A; functional years) of entering recruits is initially assigned by converting the super-individual's length to age, enabling the use of Eq. (18) to propagate length differences originating from the offspring module. Length differences are most pronounced for entering recruits and least pronounced in the terminal age class (with L close to L_∞). Mortal-

ity of parent super-individuals is the combination of natural and fishing mortality rates. Each year (Δt = 1 yr), the worth (N) of each super-individual is decreased according to natural mortality (m_n) and fishing mortality (m_f) that depends on a susceptibility (q) to harvest:

$$\Delta N = N \cdot e^{-m_n \cdot \Delta t} \cdot \left[1 - q \cdot \left(1 - e^{-m_f \cdot \Delta t}\right)\right] - N \quad (19)$$

The value of q increases as a sigmoid function of length:

$$q = \left[1 + e^{-i(L - L_{50\%})}\right]^{-1} \quad (20)$$

Once the lengths and worths of adults are updated and promoted to the next age class, they are evaluated to start the offspring for the upcoming year in the offspring module.

2.4. Assumed elevated CO_2 effects

The assumed elevated CO_2 effects were estimated from 2 types of information, species-specific and generic, and were imposed on embryos and larvae (Table 3). Flatfishes and other marine fish species appear to be more sensitive to elevated CO_2 in the very early life stages (Chambers et al. 2014, Kim et al. 2015, Pimentel et al. 2015) than as juveniles (Gräns et al. 2014, Machado et al. 2020). CO_2 effects on fertilization rate and size (length) at larval settlement were based on experimental studies of winter flounder at the NOAA Howard Marine Sciences Laboratory (R. C. Chambers unpubl. data). We added 2 generic CO_2 effects commonly demonstrated in laboratory experiments with other

Table 3. Basis for the assumed effects of elevated CO_2 on fertilization rate, size-at-settlement, mortality from developmental malformations, and larval growth rate imposed in model simulations. Fertilization and size-at-settlement were based on winter flounder data, while developmental (malformation) mortality and larval growth were generic effects based on their occurrence with many other species

Effect	Comments
Fertilization rate	Lab experiments on winter flounder; fertilization success varied with CO_2 concentration (pH from 8–7.4), and was optimal at an intermediate level (pH ~ 7.6). The odds of fertilization (i.e. the ratio of fertilized to unfertilized eggs) were approximately 3 times higher at the optimum compared to the lowest CO_2 level (pH ~ 8.0) and 1.5 times higher at the optimum compared to the highest CO_2 level (pH ~ 7.4). The *in situ* CO_2 and pH ranges experienced by winter flounder gametes in shallow embayments are unknown. We included the full range of laboratory results by assuming 80% fertilization success at the reference temperature of 5°C (Reference simulation), which was then increased to 92% (increased fertilization simulation) and decreased to 72% (decreased fertilization simulation). See Supplements 2 & 3 for additional details.
Size-at-settlement	Lab experiments on winter flounder; size-at-settlement was estimated from maximum prey consumption rates of recently metamorphosed winter flounder juveniles that had been reared from eggs in CO_2 treatments (pCO_2 of 481, 860, or 1320 µatm). We converted the measured ~20% reduction in consumption to a decrease in length-at-settlement from 8 (Reference simulation) to 7.5 mm (smaller settlement simulation), which corresponds to a ~20% reduction in mass. Measured changes in length-at-settlement (8.33–8.15 mm) were smaller than our predicted change from consumption; measured changes in length would not include all of the effects on mass, such as skinnier fish (lower condition) at settlement. See Supplement 3 for additional details.
Developmental malformations (hatching mortality)	Elevated CO_2 effects experiments in several marine fish species have demonstrated an increased occurrence of larval tissue, skeletal, and organ malformations (Frommel et al. 2012, Kim et al. 2015, Pimentel et al. 2015, 2016) and increased embryo and larval mortality rates (Baumann et al. 2012, Pimentel et al. 2016, Gobler et al. 2018). These CO_2 exposure effects were represented by adding 25% mortality at hatching (malformed simulation). Absolute CO_2 associated mortality of 25% lies near the mid-range between ~0% in *Theragra chalcogramma* (Hurst et al. 2013), *Seriola lalandi* (Watson et al. 2018), and *Cyprinodon variegatus* (DePasquale et al. 2015, Gobler et al. 2018) and ~45% in *Menidia beryllina* (averaged over Baumann et al. 2012, DePasquale et al. 2015, Gobler et al. 2018), *Paralichthys dentatus* (Chambers et al. 2014), *Argyrosomus regius*, and *Sparus aurata* (Pimentel et al. 2016). Higher increases in larval mortality have been reported for *Gadus morhua* (Stiasny et al. 2016, 2018, 2019).
Feeding larval growth	CO_2 concentrations have been shown to increase (Munday et al. 2009, Frommel et al. 2012, Chambers et al. 2014) and decrease larval growth rates (Baumann et al. 2012, Kim et al. 2015, Hurst et al. 2016). We implemented growth rate effects on feeding larvae by changing their larval digestive efficiency to obtain ~12% reduced (slower growth simulation) and ~12% increased (faster growth simulation) growth with respect to the reference simulation.

fish species. The first generic effect was implemented in the IBM as increased mortality at hatching. This was designed as a simplified representation of deleterious malformations observed in experiments that render individuals nonviable at some point between spawning and the end of the larva stage. The second generic effect was reduced or increased growth rate of feeding larvae, and was imposed as changes to digestive efficiency (this could have been done by varying metabolic rate or any bioenergetics component of growth — the change in growth rate is what affects model dynamics). While all of these assumed CO_2 effects have some empirical basis, they should be considered as speculative and illustrative of possible fish population responses, especially when imposed together on a model specific to winter flounder.

2.5. Calibration of the reference simulation

The model was calibrated using a 40 yr Reference simulation depicting conditions from 1977–2016. This Reference simulation replayed several key features of the winter population dynamics while maintaining well-known parameters at realistic values (Tables 1 & 2) and resulted in stage-, size-, and temperature-dependent growth and mortality consistent with observed data. A full description of parameter estimation and model calibration is provided in Supplement 2.

2.6. Simulation experiments

Two sets of simulation experiments were performed. The first set, termed Retrospective simulations, modeled the cumulative impact on the winter flounder population by imposing CO_2 effects on offspring every year over a 40 yr period (1977–2016). A total of 11 Retrospective simulations were performed: the Reference simulation with no CO_2 effects and 10 simulations with different combinations of CO_2 effects on offspring (Table 4). The starting population (number and length of individuals in the parent module) for each Retrospective simulation was a computed steady-state resulting from 3 repetitions of environmental data for 1977–1986 with no CO_2 effects.

Five of the 10 elevated CO_2 simulations were for combinations of the winter flounder-specific CO_2 effects of lower or higher fertilization and smaller size-at-settlement. Three simulations were for the generic CO_2 effects of increased mortality from malformations, and lower or higher digestive efficiency to generate larval growth effects. A simulation termed 'Tradeoff' paired a beneficial effect (increased growth) with a detrimental one (malformations). This pairing is commonly reported in CO_2 effects experiments (Frommel et al. 2012, Chambers et al. 2014, Kim et al. 2015, Pimentel et al. 2016, Stiasny et al. 2018). The final CO_2 simulation, termed 'Severe', was a hypothetical combination of negative effects (reduced fertilization, increased malformations, and slower larval growth rate) with smaller size-at-settlement. In addition to analyzing the entire 40 yr of output for all simulations, we further compared the Reference and Severe simulations by decade.

The second set of simulation experiments, termed Recovery simulations, explored how our assumed CO_2 effects might interact with the observed trend in ocean warming to affect population productivity. Productivity was quantified by fitting spawner–recruit (S–R) relationships to simulation results and examining the parameters of the fitted S–R curve: maximum spawning stock biomass (SSB), maximum recruitment, and steepness. Steepness is the fraction of maximum recruitment at 20% of the maximum SSB and is widely used in fishery stock assessments and management and, along with maximum SSB and

Table 4. Values of fertilization (at 5°C; for temperature effects see Table 1 and Supplement 2 & 3), size-at-settlement, increased hatching mortality related to malformations, and digestive efficiency (to adjust growth rate) used in 10 simulations of assumed effects of elevated CO_2. Size-at-settlement and fertilization were based on winter flounder data, while malformation-related (hatching) mortality and larval growth were generic effects based on their occurrence in many other species

Simulation	Fertilization (%)	Size-at-settlement (mm)	Malformation mortality (%)	Digestive efficiency (%)
Reference	80	8	0	67.5
Decreased fertilization	72	8	0	67.5
Increased fertilization	92	8	0	67.5
Smaller settlement	80	7.5	0	67.5
Smaller and decreased	72	7.5	0	67.5
Smaller and increased	92	7.5	0	67.5
Malformed	80	8	25	67.5
Slower growth	80	8	0	65
Faster growth	80	8	0	70
Tradeoff	80	8	25	70
Severe	72	7.5	25	65

recruitment, interpreted as an indicator of stock productivity (Mangel et al. 2010, Conn et al. 2010).

The Recovery simulations modeled the gradual recovery from a very low starting population to a long-term equilibrium of productivity under temperature conditions of each of the decades. For each simulation, one decade of environmental data (1977–1986, 1987–1996, 1997–2006, or 2007–2016; Decades 1 to 4, respectively) was repeated 15 times for a total of 150 yr to generate the equilibrium productivity associated with that decade. The responses in the S–R relationships are therefore the long-term consequences of each decade's temperature conditions. The Recovery experiment included only the Reference and hypothetical Severe CO_2 effects conditions. Fishing was eliminated to generate maximum rates of population recovery.

Productivity parameters (i.e. maximum SSB and recruitment) were estimated from the final 10 yr. A Beverton-Holt S–R relationship was fit to the 150 yr of simulated S–R results to estimate the steepness (Mangel et. al. 2010). The S–R relationships were compared between the Reference and hypothetical Severe CO_2 conditions for each of the 4 decades to assess whether CO_2 effects interact with effects from warming conditions to impact population productivity (warmer Decades 3 and 4 vs. the cooler Decades 1 and 2).

2.7. Model outputs

A variety of model outputs were used to characterize the simulated population dynamics of winter flounder in the Retrospective and Recovery simulation experiments (Table 5). The main results of the 2 simulation experiments are reported here (see Supplements 2, 4 & 5 for additional results and calibra-

Table 5. Model output variables used in the analysis of the Retrospective and Recovery simulation experiments. SSB: spawning stock biomass; YOY: young-of-the-year; S–R: spawner–recruit

Variable	Units	Description
Spawning day	Ordinal day	Average day that embryos are initiated over all parents
Duration	Days	Average days spent by individuals surviving a stage
Survival fraction	Proportion	Proportion of entering individuals that exit a stage
Recruitment	No. of individuals	Number of YOY juvenile individuals on 31 Dec; will enter parent module as age-1
Recruits per embryo	Proportion	Proportion of overall survival through YOY stages; cumulative effects of stage-specific survivals
Body mass	g	Final average dry mass of YOY juveniles on 31 Dec; reflects any effects on bioenergetics and growth
Body length	mm	Final average length of YOY juveniles on 31 Dec; reflects effects of growth and parent module uses length-based growth and mortality
SSB	kt	Summed wet mass of mature adult individuals on 21 Aug; proxy for reproduction potential
Fraction mature of age-3[a]	Proportion	Proportion mature based on interpolated length at onset of spawning (P in Eq. 2) for age-3. Age-3 is when year-class productivity peaks and when the lagged effects of recruit body mass and length have the strongest effects on maturity and fecundity
Embryos per age-3[a]	Unitless	Number of fertilized embryos per age-3 female individual. Age-3 is when year-class productivity peaks and when the lagged effects of recruit body mass and length have the strongest effects on maturity and fecundity
Maximum SSB	kt	Averaged SSB in the final 10 yr of recovery simulations without fishing; used as a measure of productivity and to estimate steepness of S–R relationship
Maximum recruitment	No. of individuals	Averaged recruitment in the final 10 yr of recovery simulations without fishing; used as a measure of productivity and to estimate steepness of S–R relationship
Steepness	Unitless	Fraction of maximum recruitment at 20% of the maximum SSB

[a]Labeled as age-3 because they are approximately 3 yr old at spawning; they became age-2 in the parent module on 21 August of the previous year

tion method). Percentage deviation from Reference simulation values are shown for many of the outputs $[(Y - Y_{ref}) / Y_{ref} \cdot 100]$ (absolute deviation values are in Supplement 5). To clarify model output nomenclature, parent module SSB labeled as year 1980 reflects growth and mortality from 21 August 1979 to 20 August 1980 and generates offspring module spawning (during January to March) and recruitment (31 December) labeled as 1981.

3. RESULTS

3.1. Reference simulation

In the Reference simulation, averaged SSB was similar (~37 kt) throughout the first 3 decades (i.e. 1977–2006), but dropped precipitously in the last decade (26.3 kt; Fig. 3). The maximum SSB (42.9 kt in 2001) was similar to the target SSB value of 44 kt estimated in a recent stock assessment (NEFSC 2011). The final SSB (20.9 kt in 2016), which was also the minimum SSB, was only 56% of the 1977–2006 average. Simulated annual recruitment showed a similar trend as SSB but with more inter-annual variability, indicating years with particularly favorable (e.g. 1996) and unfavorable (e.g. 1995) temperature conditions in the offspring module (Fig. 4). Annual recruitment ranged from 45.8–105.9 million individuals during the first 3 decades, peaked a few years earlier than SSB (1997 vs. 2002), and followed a steep declining trend for the remaining years. By the final decade, averaged recruitment had dropped by about half since the first 2 decades (36.0 vs. 70.0 and 72.5 × 10^6).

Average annual temperatures by decade were 11.4, 11.6, 12.1, and 12.6°C (Decades 1 to 4, respectively), with similar ranges across decades when viewed month-by-month (Fig. 1). Approximately half of the interannual variability in survival from spawning to recruitment (recruits per embryo) was explained by variability in the annual mean temperature (R^2 = 47%, Kendall Tau = −49%, $p < 0.0001$; Fig. 5). The warming trend in the Reference simulation also caused a marked decline in productivity (Fig. 6). In the Decades 1 and 2, recruitment was about equally likely to fall below or above that predicted by the S–R relationship used to calibrate the model (9 and 11 yr, respectively). In Decades 3 and 4, recruitment was consistently below that predicted by

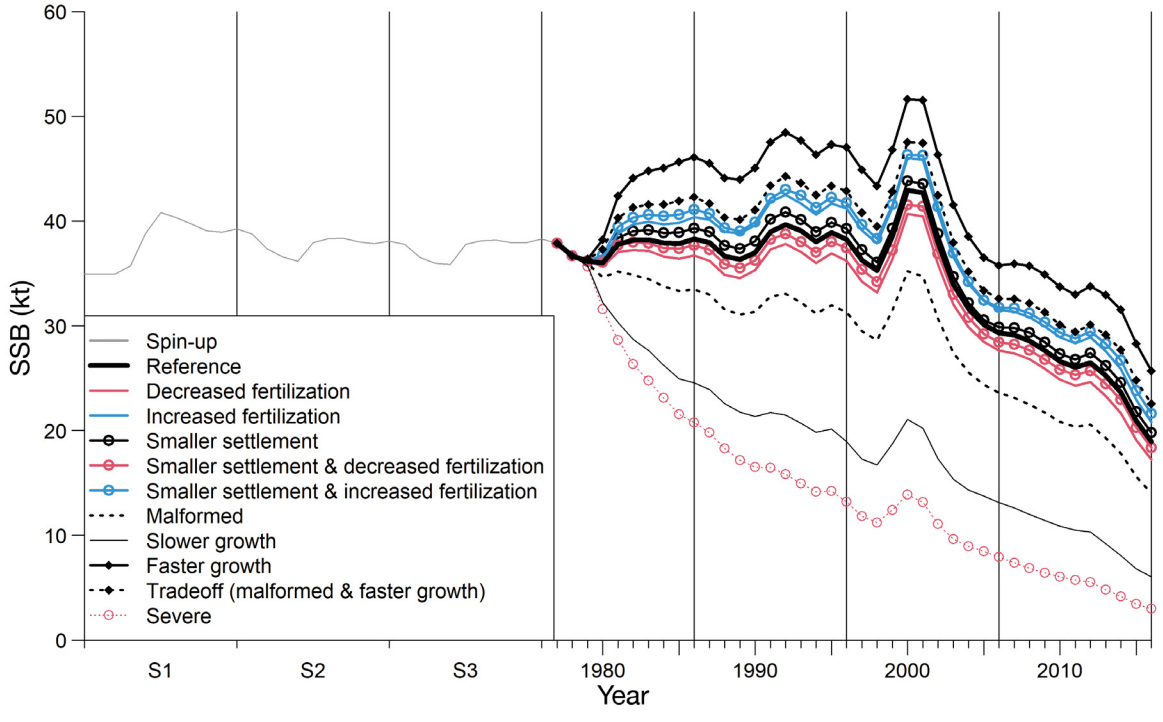

Fig. 3. Annual projected spawning stock biomass (SSB) during a spin-up period (S1–S3) and then for 1977–2016 for the Reference simulation and 10 simulations with assumed effects of elevated CO_2. The spin-up period is 3 repetitions of the environmental conditions of Decade 1 under reference (no elevated CO_2 effects) conditions. The assumed CO_2 effects for these simulations are described in Table 4. The effects are single and combinations of changes in fertilization, size-at-settelment, malformation-related mortality (imposed at hatching), and changed larval growth (digestive efficiency)

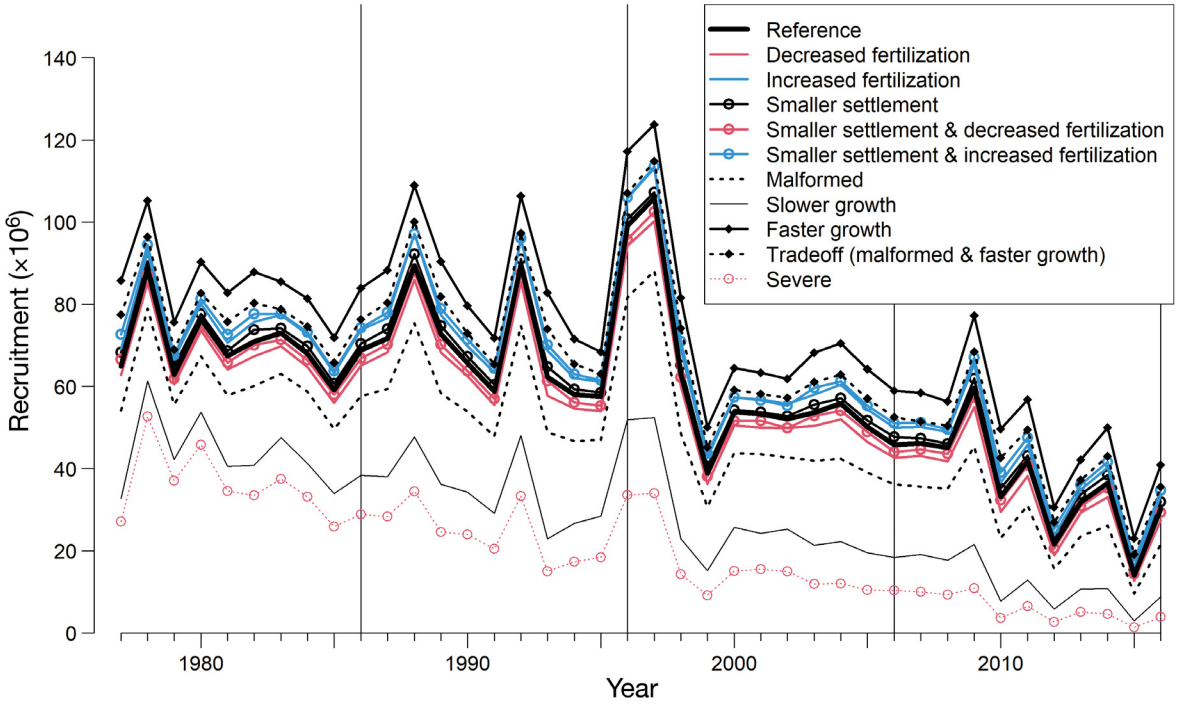

Fig. 4. Annual projected recruitment of YOY juveniles for 1977 through 2016 for the Reference simulation and 10 simulations with the assumed CO_2 effects. Layout as in Fig. 3 but with spin-up omitted here

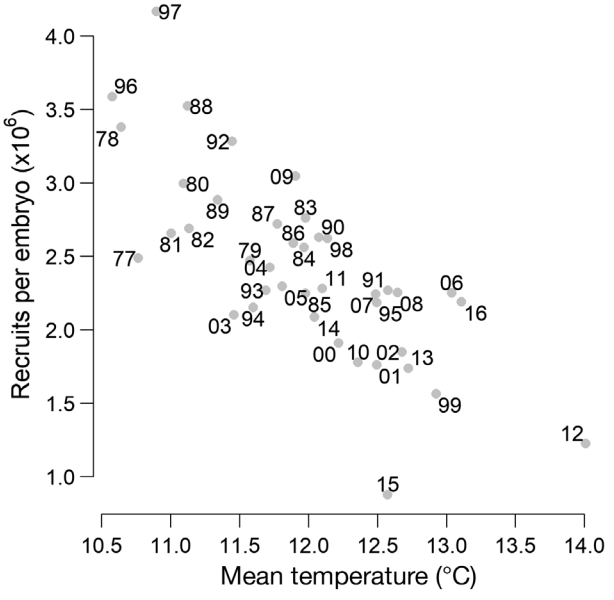

Fig. 5. Relationship between recruits per embryo and annual mean temperature from the Reference simulation for 1977–2016 (numerals indicate year)

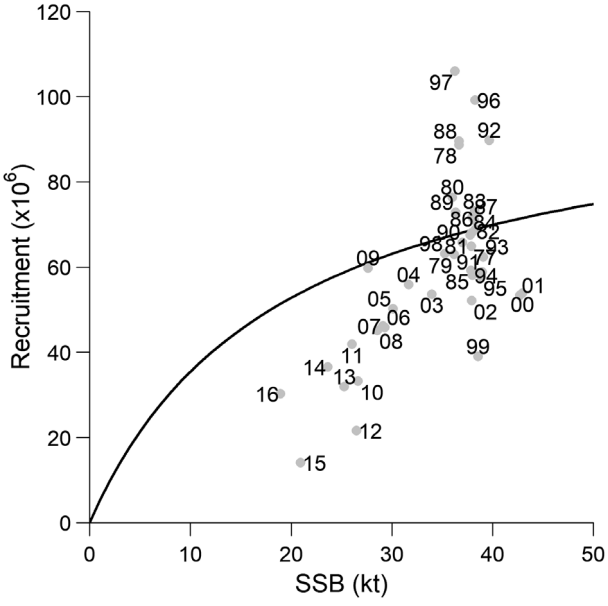

Fig. 6. Spawner–recruit results from the Reference simulation for 1977–2016. Points are labeled by the year of YOY dynamics leading to recruitment at the end of that year. The calibration (curve) is based on a recent winter flounder stock assessment (NEFSC 2011). SSB: spawning stock biomass

the S–R relationship (19 of 20 yr; binomial test, $p < 0.0001$). The S–R relationship reported in a recent stock assessment (NEFSC 2011) and used for calibration here was based on a 30 yr subset (1981–2010) of the simulated time period that included cool and warm years, but did not include environmental covariates in the S–R relationship.

Table 6. Model outputs averaged by decade for the 40 yr Reference simulation. Spawning day is set by temperature effects on oocyte and ova development. YOY dynamics are summarized by stage duration, stage survival (fraction), body size (mass, length) at recruitment, recruitment, and recruit per embryo. Adult dynamics are summarized by spawning stock biomass (SSB), percent of age-3 mature, and embryos per individual of age 3

Output	Stage	Overall	Decade			
			1	2	3	4
Spawning day (ordinal d)	Embryo	72.8	80.0	76.2	71.8	63.3
Duration (d)	Embryo	18.0	18.4	17.6	17.7	18.4
	Yolk-sac larva	7.5	7.5	7.4	7.5	7.7
	Feeding larva	39.2	38.4	38.9	39.3	40.5
	Settle to 31 Dec	227.1	220.1	224.3	228.5	235.3
Survival fraction	Embryo	0.106	0.103	0.108	0.108	0.105
	Yolk-sac larva	0.428	0.429	0.430	0.428	0.426
	Feeding larva	0.0152	0.0152	0.0154	0.0154	0.0147
	Settle to 31 Dec	0.00356	0.00407	0.00392	0.00323	0.00303
Body mass (g)	31 Dec	1.06	1.07	1.13	1.05	0.98
Body length (mm)	31 Dec	85.96	86.25	87.74	85.80	84.05
Recruits per embryo ($\times 10^{-6}$)	Embryo to 31 Dec	2.423	2.682	2.789	2.293	1.971
Recruitment ($\times 10^{6}$)	31 Dec	59.0	70.0	72.5	57.3	36.0
SSB (kt)	Adult	34.6	37.5	38.0	36.7	26.3
Percent of age-3 mature	Ova	37.2	38.1	38.6	36.8	35.3
Embryos per age-3 ($\times 10^{5}$)	Embryo	1.43	1.49	1.50	1.40	1.32

Table 7. Average temperature (°C) by decade experienced by each life stage within the YOY for the Reference simulation

Stage	Decade			
	1	2	3	4
Ova	3.0	3.6	3.8	3.9
Embryo	4.9	5.1	5.1	4.9
Yolk-sac larva	6.2	6.2	6.1	5.9
Feeding larva	8.9	8.7	8.5	8.3
Settle to 31 Dec	15.6	15.5	16.0	16.4

Warming over the course of the Reference simulation caused earlier spawning and resulted in longer stage duration, slower growth, and reduced survival of the post-embryonic life stages (Table 6). Despite the inter-decadal warming trend, only some life stages were exposed to warmer temperatures in later decades (Table 7). Key to these results is that warming temperatures accelerated oocyte and ova development, which led to earlier spawning (Table 6). The mean spawning day relative to the first decade was 3.8 d earlier in Decade 2, 8.3 d in Decade 3, and 16.8 d in Decade 4. As a consequence of earlier spawning, the embryonic stage experienced little net change in water temperature, while the yolk-sac larval and feeding larval stages experienced cooler water temperatures (contributing to slower growth) in warmer decades (Table 7). Juveniles experienced a net increase in temperature in warmer decades, including temperatures above the range supporting high consumption and growth. Earlier spawning and slower growth resulted in a gradual increase, from Decade 1 to Decade 4, in the stage durations for feeding larvae (from 38.4 to 40.5 d) and juveniles (from 227.1 to 235.3 d) (Table 6). As a consequence of longer stage duration, there was a slight decrease in stage survival for feeding larvae by Decade 4 (0.0147 vs. 0.0152–0.0154 in earlier decades). For juveniles, the combination of longer stage durations and warmer temperatures resulted in a substantial decrease in stage survival from Decade 1 (0.0041) to Decade 4 (0.0030). This decrease in juvenile survival occurred despite the opposing effect of reduced density-dependent mortality with population decline. Overall survival, summarized by the recruits per embryo ($\times 10^{-6}$) was high in Decades 1 and 2 (2.682 and 2.789), dropped in Decade 3 (2.293), and dropped again in Decade 4 (1.971).

Juveniles surviving to 31 December (recruits) also decreased in size from Decades 1 and 2 (mean mass: ≥1.07 g; mean length: ≥86.25 mm) to Decade 4 (0.98 g; 84.05 mm). While the negative effects of warming on survival during the first year of life had major consequences for reduced SSB and recruitment, the negative warming effects on growth of YOY indi-

viduals had only minor consequences for the size-dependent processes (e.g. maturity, fecundity) of the adults. The difference between 0.98 g (Decade 4) and 1.13 g (Decade 2) dry mass on 31 Dec is equivalent to a 10.5 d delay in growth and maturation of adults. Fecundity at age-3 (embryos per individual × 10^5) was higher in the 2 earlier, cooler decades (1.48–1.51) and lowest in the final, warmest decade (1.33). This reduction in fecundity of ~10% was due to the smaller size of recruits during warm periods combined with less growth opportunity for subadults (due to earlier spawning dates) resulting in a smaller size of adults. Over time, the smaller size at spawning resulted in less fecund adults at age-3 (5.03, 5.04, 4.94, and 4.84 × 10^5, Decades 1 to 4, respectively) and a decreased probability of maturity by age-3 (0.38, 0.39, 0.37, and 0.35, Decades 1 to 4, respectively). The combination of reduced fecundity and fewer mature fish at age-3 accounted for the ~10% reduction in the total age-3 fecundity over time.

3.2. Retrospective experiment: population responses to potential elevated CO_2 effects

The assumed generic CO_2 effects (mortality due to developmental malformations and growth) had larger population impacts than the assumed CO_2 effects based on winter flounder experiments (egg fertilization rate, size-at-settlement) (Figs. 3 & 4, Table 8). Reduced fertilization and smaller size-at-settlement, alone and in combinations, resulted in changes of <±8% in the 40 yr average SSB compared to the Reference simulation. Malformation alone and the Tradeoff (malformation with increased growth) had larger impacts (–14.9 and +10.0%) on the 40 yr average SSB. Among all CO_2 effects, variation in larval growth (either increase or decrease) had the largest individual effect on SSB (–41.2 and +19.3%). When all negative effects plus smaller size-at-settlement (which has tentative species-specific evidence) were considered together (i.e. Severe condition), SSB was reduced by 53.5% from Reference simulation values.

For each CO_2 effect considered, the directly impacted life stages showed large (>±10%) changes in survival compared to Reference simulation values. Since all of these effects occurred before the juvenile stage (i.e. prior to settlement), they were partially compensated by changes in density-dependent juvenile mortality. With density-dependent mortality, increased juvenile densities due to increased pre-juvenile survival led to decreased juvenile stage survival. For example, modeled changes to fertilization rate (–10 and +15%), which changed survival from the ova stage to the embryo stage, triggered counteracting responses in juvenile stage survival (+8.3 and –11.3%, respectively). Similarly, the CO_2 effect of smaller size-at-settlement resulted in a shortened larval stage duration and an increase in larval stage survival by 22% relative to Reference values. This

Table 8. Percentage change of young-of-the-year and adult outputs between each of the elevated CO_2 simulations and the Reference simulation over the entire 40 yr of simulations in the Retrospective experiment. Percent change is computed as: $(Y - Y_{ref})/Y_{ref} \cdot 100$; only changes greater than 1% are shown. The assumed CO_2 effects for these simulations are described in Table 4

	Fertilization		Smaller settlement and fert.			Mal-	Growth		Trade-	Severe
	Decr.	Incr.	Same	Decr.	Incr.	formed	Slower	Faster	off	
Duration										
Embryo										
Yolk-sac larva										
Feeding larva			–6.4	–6.4	–6.4		14.2	–10.8	–10.7	6.9
Settle to 31 Dec							–1.5		1.3	
Survival fraction										
Embryo						–24.6			–24.8	–24.8
Yolk-sac larva										
Feeding larva			22.0	22.0	21.7		–50.9	67.2	67.5	–37.7
Settle to 31 Dec	8.3	–11.3	–17.5	–10	–26.9	27.1	70.6	–37.8	–18.8	75.6
Body mass on 31 Dec			1.3	1.4			–4.0	2.7	3.7	–1.9
Body length on 31 Dec							–1.2		1.1	
Recruits per embryo	8.9	–11.4		9.9	–10.9	–4.5	–16.0	5.0	2.7	–17.2
Recruitment	–5.7	7.5	2.8	–2.5	9.3	–18.5	–50.8	24.2	12.4	–65.6
SSB	–4.5	6.0	2.2	–2.0	7.3	–14.9	–41.2	19.3	10.0	–53.5
Percent of age-3 mature										
Embryos per age-3	–9.5	14.3		–9.2	14.6					–9.6

increase in supply of juveniles from the larval stage was mostly offset by lower juvenile stage survival (–17.5%) due to its density-dependent mortality. When fertilization and size-at-settlement effects were combined, the expected direct effects and compensatory responses by juvenile stage survival resulted in net changes in average SSB of –2.0% (for reduced fertilization) and +7.3% (for increased fertilization). Similarly, the CO_2 effect on embryo malformation and hatching survival (–24.6%) was partially offset by increased juvenile stage survival (+27.1%), resulting in a 14.9% (rather than 24.6%) reduction in average SSB.

CO_2-induced growth effects in feeding larvae had the largest direct impacts. Completing the larval stage at a reduced growth rate (~88% of Reference) predictably resulted in a protracted stage duration $\left(\frac{100\%}{88\%} \approx 114\%\right)$, whereas a faster growth rate (~112% compared to Reference) resulted in shortened stage duration $\left(\frac{100\%}{112\%} \approx 89\%\right)$. The compounding effects of daily length-dependent mortality strongly amplified these changes in stage duration, resulting in large changes in larval stage survival (–50.9 and +67.2% survival fraction, respectively). Again, compensatory changes in density-dependent juvenile survival (+70.1 and –37.8%, respectively) partially offset these direct impacts. The hypothetical combined CO_2 effects in the Severe simulation (Table 4) had the expected direct effects of reduced life stage survival and, despite a large counteracting increase in juvenile stage survival due to density release (+75.6%), resulted in a large reduction (–53.5%) in average SSB.

Changes in survival due to altered fertilization rate, hatching mortality, and larval growth were carried over to changes in SSB with a predictable, asymmetrical amount of dampening. The causes of dampening were primarily compensatory density-dependent juvenile mortality and secondarily the time lag from how survival effects on early life stages manifest in lifetime reproductive output of the affected individuals. Large increases in survival were more severely dampened while large decreases in survival were only slightly offset. For example, 51% fewer individuals surviving the larval stage due to slow growth resulted in 41% lower SSB than in Reference (1–0.41/0.51 or 21% dampening), and 25% fewer individuals entering the embryo stage due to malformations resulted in 15% lower SSB (40% dampening). In comparison, 15% more embryos from increased fertilization resulted in only 6% higher SSB (15 vs. 6% or a large 60% dampening), and 67% more surviving larvae due to faster growth resulted in the relatively small 19% higher SSB (also a large 71% dampening). The asymmetric dampening pattern is a result of the interplay among the life stage dynamics during the first year of life and is summarized in the model-generated stock–recruitment relationship (see Fig. 6). The simulated Reference population is situated on the S–R curve where the curvature of the relationship shows how reduced population (SSB) due to reduced survival generates larger reductions in recruitment than higher population size (from increased survival) generates increased recruitment.

Average recruitment tracked the changes in average SSB, while recruits per embryo sometimes changed in the opposite direction (Table 6). Recruits per embryo is influenced by all direct CO_2 effects on embryos and larvae as well as density-dependent mortality of juveniles, but not changes in SSB. The 2 metrics had opposite signs when changes were relatively small (fertilization and size-at-settlement), and had the same sign when changes were large (malformed, growth, Tradeoff, and Severe conditions). Opposite signs occurred when the compensatory release from density-dependence was sufficient to offset annual direct CO_2 effects, but not the cumulative effects on SSB. The fraction mature and fecundity at age-3 did not vary more than 1% from Reference values across all simulations (Table 8).

3.3. Retrospective experiment: time course of population responses

Despite warming through the decades, the population-level responses to elevated CO_2 were consistent among the 4 decades. Responses in duration and survival for the life stages directly affected were nearly constant when expressed as changes relative to Reference simulation values for the same decade. Even in the Severe scenario, stage durations and pre-juvenile stage survival relative to Reference simulations varied little by decade (Table 9). For example, in all 4 decades, the larval stage survival in the Severe scenario was about 40% lower compared to the Reference simulation. Responses in the juvenile stage were more variable because of density-dependent mortality.

With respect to SSB and recruitment, the impacts of the assumed CO_2 effects accumulated over time (Figs. 3 & 4) but showed similar impacts across decades. For example, average SSB in the Severe simulation fell from 16.80 kt in Decade 2 to 11.37 kt in Decade 3. This decrease was in part due to negative

Table 9. Percentage changes in YOY and adult outputs averaged by decade between the Severe elevated CO_2 simulation and the Reference simulation as part of the Retrospective experiment. Percentage change is computed as: $(Y - Y_{ref})/Y_{ref} \cdot 100$; only changes greater than 1% are shown

Output	Stage	Decade			
		1	2	3	4
Duration (d)	Embryo Yolk-sac larva Feeding larva Settle to 31 Dec	7.2	6.9	7.0	6.5
Survival fraction	Embryo Yolk-sac larva Foraging larvae Settle to 31 Dec	−24.9 −38.3 55.8	−24.9 −37.9 87.3	−24.9 −37.6 93.9	−24.5 −37.2 67.5
Body mass (g)	31 Dec	−2.0	−1.3	−1.3	−2.8
Body length (mm)	31 Dec				
Recruits per embryo	Embryo to 31 Dec	−28.0	−12.1	−8.4	−19.9
Percent of age-3 mature	Ova				
Embryos per age-3	Embryo	−10.3	−9.8	−9.2	−9.1

CO_2 effects during Decade 3 (1997–2006), but also because SSB at the beginning of Decade 3 was already much lower than at the beginning of Decade 2 (14.22 vs. 21.55 kt) from CO_2 effects operating during the first 2 decades. Recruitment also showed similar accumulation of elevated CO_2 effects (Fig. 4). However, overall YOY survival (recruits per embryo) and reproduction (embryos per age-3 females) each showed similar percentage reductions across decades despite declining SSB and recruitment and warming (Table 9). The fraction of fish mature at age-3 relative to the Reference simulation values also did not vary across decades.

3.4. Recovery experiment

Many repetitions of the environmental conditions of each decade showed that, although not apparent in the Retrospective experiment, warming amplified the assumed effects of elevated CO_2 conditions on long-term population productivity (Fig. 7). For each decade, annual SSB rose through time from the low initial value to an unfished equilibrium. Population recovery was more sensitive to the hypothetical Severe CO_2 effects than historic warming alone. All 4 simulations (corresponding to repetitions of each decade) with Severe CO_2 effects showed increases in SSB that lagged (slower recovery) behind even the warmest decade (worst thermal conditions) without CO_2 effects (Fig. 7).

Under equilibrium conditions, maximum SSB and recruitment showed similar patterns across decades. Maximum SSB was highest in Decades 1 and 2 (134.5 and 136.3 kt), intermediate in Decade 3 (105.4 kt), and lowest in Decade 4 (72.4 kt) (Table 10). Maximum recruitment ($\times 10^6$) similarly went from 98.6 and 104.4 in Decades 1 and 2 to 73.5 in Decade 3 and 36.3 in Decade 4 (Table 10). The reductions in SSB and maximum recruitment from Reference to Severe simulations were the same within each decade but increased from one decade to the next (27, 24, 30, and 50% for Decades 1–4, respectively). Thus, warming increased the negative effects of the Severe CO_2 effects on maximum SSB and recruitment.

All 4 decades had similarly high estimates of steepness for the Reference simulations (0.56–0.66) and similarly low estimates of steepness for the Severe CO_2 simulations (0.35–0.42) (Table 10). Severe CO_2 effects greatly exacerbated the lowered population productivity caused by warming. The fitted S–R relationships were lower and truncated on the right (reaching lower equilibrium SSB) with warming (Fig. 8A) and even further shifted and truncated with warming and assumed CO_2 effects (Fig. 8B).

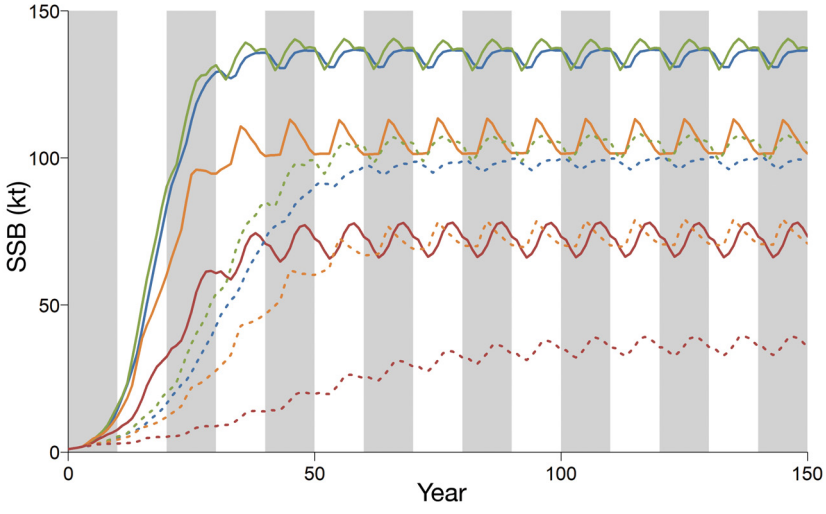

Fig. 7. Projected annual spawning stock biomass (SSB) for the Reference (solid) and hypothetical Severe CO_2 (dashed) simulations for each decade of environmental data in the Recovery experiment. Blue: 1977–1986; green: 1987–1996; orange: 1997–2006; red: 2007–2016

Table 10. Maximum spawning stock biomass (SSB) and maximum recruitment of age-1 to the parent module (both as 10 yr averages), and derived steepness of the fitted spawner–recruit curve for each decade (repeated 15 times) of environmental data in the Recovery experiment.

Decade	Maximum SSB (kt)		Maximum recruitment ($\times 10^6$)		Steepness	
	Reference	Severe	Reference	Severe	Reference	Severe
1	134.5	98.6	98.7	72.2	0.66	0.38
2	136.3	104.4	99.6	76.1	0.63	0.42
3	105.4	73.5	77.5	53.9	0.60	0.38
4	72.4	36.3	53.4	26.6	0.56	0.35

4. DISCUSSION

Assessing the effects of elevated CO_2 at the population and higher levels has long been a shared goal among OA researchers (Le Quesne & Pinnegar 2012, Andersson et al. 2015, Gaylord et al. 2015). We used an IBM approach to simulate the population dynamics of winter flounder through a multi-decadal series of warming temperatures under a range of assumptions about possible effects of elevated CO_2. The IBM approach has been suggested for OA effects modeling (Koenigstein et al. 2016) and is now widely used to simulate population dynamics of fish and other taxa (DeAngelis & Grimm 2014). Our model built off an earlier IBM effort for winter flounder at the same location (Chambers et al. 1995, Rose et al. 1996, Tyler et al. 1997) but was highly modified to include CO_2 effects on fertilization, survival, growth, and size-at-settlement.

The winter flounder is a good candidate for our study because it is well studied (Pereira et al. 1999, Lorda et al. 2000), is categorized as very highly vulnerable to climate exposure, and is also considered to have high biological sensitivity (Hare et al. 2016). Although there are many examples of wide-ranging CO_2 effects in marine taxa, including aspects of behavior and sensory capabilities (Clements & Hunt 2015, Cattano et al. 2018), our analysis focused on commonly observed effects on growth, development, and mortality during the early life stages. To explore legacy population-level effects from early life stages, we coupled a detailed offspring module to a simpler approach for age-1 and older individuals (parent module). Our simplifying assumption of a single spa-

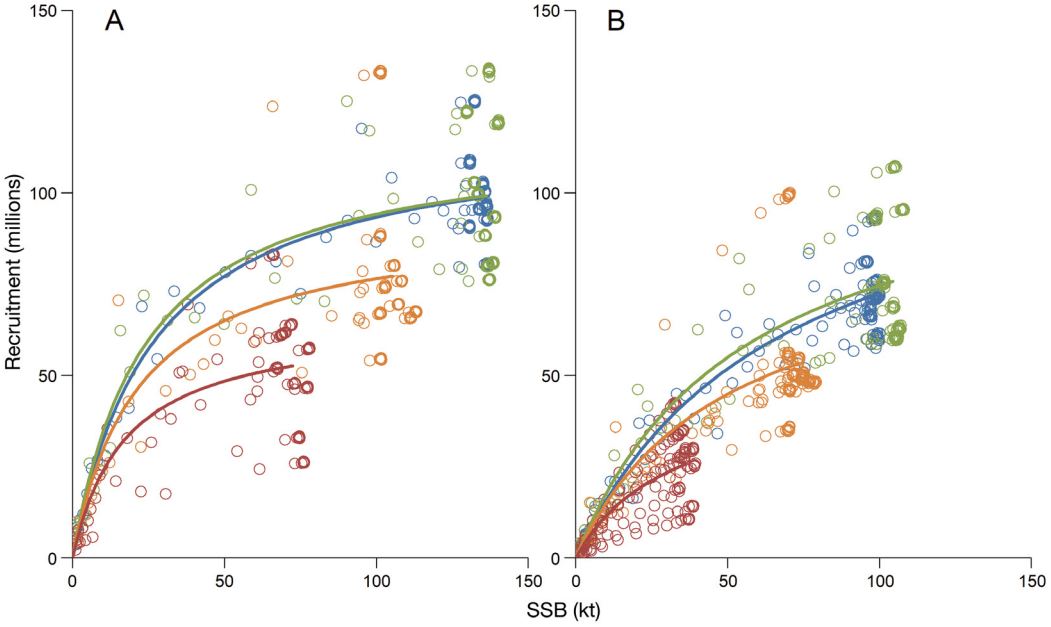

Fig. 8. Beverton Holt spawner–recruit relationships fit to spawners and recruits generated for each decade of environmental data in the Recovery experiment. (A) Reference simulation and (B) hypothetical Severe CO_2 simulation. Blue: 1977–1986; green: 1987–1996; orange: 1997–2006; red: 2007–2016; SSB: spawning stock biomass

tial box for full life-cycle simulations is reasonable for winter flounder because adults spawn in the same estuarine habitats where the early life stages reside during their first year of life (Klein-MacPhee 1978; see Supplement 2). This coupled modeling approach simulated how effects in the first year of life might translate to longer term population responses.

4.1. Interpretation and implications of our results

Warming temperatures were found to have a major negative effect on the simulated winter flounder population. In the Reference simulation, we traced long-term (40 yr) effects of warming, which included a cascade of impacts beginning with earlier spawning and the occurrence of embryos and subsequent life stages earlier in the year, followed by exposure to temperatures unfavorable for growth (too cool for larvae, too warm for juveniles), resulting in extended life stage durations, and ultimately causing lower YOY survival. Recruits-per-embryo was lowest in the last decade of these 40 yr projections. This pattern is consistent with field evidence. Able et al. (2014) analyzed field data for winter flounder during 1980–2010 and identified that warm springs consistently resulted in reduced recruitment. Warm summer temperatures frequently coincide with reduced juvenile growth (Sogard 1992, Meng et al. 2000, Manderson et al. 2002).

In our simulations, the effects of warming on growth during the early life history, culminating in reduced sizes of recruits, were small and did not dramatically alter the subsequent dynamics of the adult population. Nevertheless, average recruitment was reduced by 45% by Decade 4 compared to Decade 1 (36.0 vs. 70.0 × 10^6), and this was reflected in a reduction in mean SSB of ~30% (Table 6).

Among the assumed CO_2 effects considered here, reduced growth of feeding larvae had the largest single-factor impact on the simulated winter flounder population. Average recruitment was reduced by 50.8% and average SSB was reduced by 41.2% over the 40 yr relative to the Reference simulation (Table 8). Of the remaining elevated CO_2 effects, mortality from malformations had moderate consequences, whereas effects on fertilization and size-at-settlement had smaller consequences. The ultimate population consequences of the assumed CO_2 effects were partially offset by density-dependent juvenile mortality. This caused an increase in juvenile survival when the mortality of earlier life stages was higher. Importantly, the largest reductions in recruitment (–65.6%) and SSB (–53.5%) occurred for our hypothetical combination of multiple CO_2 effects. This was called the Severe simulation here, but the occurrence of multiple CO_2 effects *in situ* seems likely, due to a common underlying physiological basis of CO_2 responses. Analysis of the Reference and Severe simulations by decade showed that the direct effects of the Severe CO_2 conditions were not amplified by warming (Table 9).

Our Recovery simulation experiment showed how warming and our hypothetical combination of Severe CO_2 effects can interact in a synergistic way to negatively affect population productivity. We used model simulations to estimate decade-specific S–R relationships. Representation of density-dependent mortality (and other processes) in population dynamics models is a long-standing challenge but is necessary to realistically simulate long-term population dynamics (Rose et al. 2001). In our model, the mechanism for population resilience was density-dependent survival of juveniles. Density dependence dampens the effect of warming and the negative (as well as positive) effects of elevated CO_2. Besides winter flounder (DeLong et al. 2001), density-dependent mortality has been described for the juvenile stage in many finfish species and especially in other flatfish, which metamorphose from a pelagic larva inhabiting a 3-dimensional habitat to benthic juveniles occupying a 2-dimensional one (Myers & Cadigan 1993, van der Veer et al. 2000). Natural mortality of adults is generally assumed to be density-independent in winter flounder (e.g. NEFSC 2011) and species with similar life history (Rose et al. 2001), although some evidence exists for density dependence in adult growth, mortality, and reproduction for some species (Lorenzen & Enberg 2002), including flatfish (Rijnsdorp 1994). Further analyses should address how density dependence in adults modifies the simulated population responses here.

The results of the Recovery experiment illustrated how effects of elevated CO_2 might amplify negative effects of warming on population productivity. Maximum SSB and maximum recruitment decreased with warming alone (Reference conditions; Table 10). For example, maximum SSB and recruitment both decreased by about 45% (134.5–72.4 mt; 98.7–53.4 × 10^6) from Decades 1–4. When the hypothetical Severe CO_2 effects were added to warming effects (Table 10), maximum SSB and recruitment between Decades 1 and 4 were both reduced by about 63% (vs. 45% in Reference). This synergistic effect was not apparent in the Retrospective experiment, likely due to the shorter duration of the simulation, smaller range of

values of SSB, and populations that were in sharp decline at the end of the simulation as opposed to being in equilibrium. The 33–42% decrease in S–R relationship steepness caused by assumed CO_2 effects in each of the 4 decades did not depend on warming. With declining productivity, the years used to estimate the S–R relationship become critical so as to not overestimate the productivity of the stock into the future.

A cautionary note is that the model-generated steepness values, especially in Decade 4 with Severe CO_2 conditions (0.35–0.42), were lower than reported values and, while reflective of the Severe effects within our virtual world, are unrealistic (see Rose et al. 2001). Shertzer & Conn (2012) and Midway et al. (2018) included values of steepness as low as 0.2 in their analyses for flatfish but noted that these were included as extremely low values to illustrate their analyses. Our values of steepness are meant for comparison of relative changes among simulations and do not represent empirically based realistic values in absolute terms and are not intended for management use.

Our result that uncertain OA effects could range from dramatic and exacerbating to partially compensating better-understood temperature effects has been extensively discussed by others (Gobler et al. 2018, Watson et al. 2018, Baumann 2019). Field studies and analysis of long-term monitoring data also have shown declines in winter flounder on the northeast coast of the USA, likely due to warming temperatures (Able et al. 2014, Bell et al. 2014). While future climate scenarios were not explicitly modeled here, the historical temperature data offered a test of warming effects because of general warming of about 1.2°C that occurred between 1977 and 2016. Our simulated decline in winter flounder for the Reference simulation of the Retrospective experiment seems reasonable in this context.

The Severe simulation used in the Retrospective and Recovery experiments should not be interpreted as a realistic worst-case scenario. By including 4 different CO_2 effects, the Severe simulation allowed us to explore how multiple effects on multiple stages translate to population-level responses. We did not scrutinize whether multiple individual effects would realistically occur together in a single location or whether effects on earlier stages would affect the sensitivity of later stages by culling more sensitive or susceptible individuals. Further specificity of OA effects on winter flounder tailored to a location and benchmarked to a specific climate change scenario would allow for better assessment of expected and worst-case conditions.

4.2. Testing several key model assumptions

As with any complex model, a number of assumptions were made here, and 2 specific assumptions related to temperature effects warrant further comment. The assumption that temperature-dependent oocyte and ova development would act to adjust the timing of spawning resulted in spawning earlier in the year but at similar temperatures in all 4 decades. To test the influence of this assumption, we repeated the Reference and Severe CO_2 simulations of the Retrospective experiment but with timing of spawning fixed for all decades reflecting the spawning dates exhibited in Decade 1. The effects of warming on average SSB with fixed spawning were similar to the original Reference simulation results and the assumed effects of elevated CO_2 were also similar (Supplement 4). For example, the reductions of averaged SSB between the Reference and fixed spawning simulations were 18.8 versus 18.6% in Decade 1 and 77.9 versus 84.5% in Decade 4.

A second temperature-related assumption was the dependence of embryonic through juvenile mortality rate on temperature (Q_m in Eq. 16). Field observations support the assumption of elevated mortality during summer and warmer years. This appears to be especially true in the warmer, southerly reaches of the geographic range, and indirect negative effects of the predatory guild during warmer years may also play a role (Jeffries & Terceiro 1985, Taylor 2005). To assess the importance of our temperature-related mortality assumption, we eliminated the temperature effects (i.e. set $Q_m = 1.0$) and repeated the Reference and Severe CO_2 simulations (Supplement 4). Predicted reductions in averaged SSB due to warming and due to the hypothetical combination in the Severe effects by decade were also comparable to those obtained with the original temperature-dependent mortality. Averaged reductions in SSB for the original Reference versus temperature-independent morality version of the Reference simulation were 18.8 versus 16.2% in Decade 1 and 77.9 versus 75.6% in Decade 4.

The representation here of elevated CO_2 concentrations and effects requires further investigation. Regarding CO_2 concentrations, values employed in laboratory studies used to inform the IBM were between 800 and 2000 µatm CO_2. Rather than using responses in the model drawn from a simple, dichotomous, present–absent depiction, we recommend that the responses to elevated CO_2 be quantified over a wider range of CO_2 concentrations and with more finely parsed treatment levels in order to provide a

robust functional form of the response. Elevated CO_2 concentrations used to quantify biological effects should also be allowed to vary at seasonal or even higher temporal frequencies, as this would more accurately reflect reported patterns of estuaries such as those used by winter flounder (Baumann et al. 2015) and other coastal fishes (Potter et al. 2015). Use of OA conditions from other models under specific IPCC scenarios, as done with some other population modeling (e.g. Koenigstein et al. 2018), would improve the realism of our simulations. Our model forced all individuals to experience the warming and elevated CO_2 conditions. We did not allow behavior to modify the thermal and CO_2 regimes experienced by individual fish, e.g. movement or migration in response to CO_2 or temperature (Nye et al. 2009, Ziegler et al. 2018). Lastly, our model ignored plasticity, acclimation, and the potential for adaptation (Hofmann et al. 2010, Gaylord et al. 2015, Nagelkerken & Munday 2016).

4.3. Generality of our results

Relatively few previous studies have used models to simulate population-level responses to warming temperatures and OA effects (elevated CO_2) alone and in combination; we summarize representative examples below, including an analysis at the level of the food web, and compare results for fish with our simulated responses of winter flounder.

Several analyses have attempted to predict changes in life-history parameters (e.g. growth rate, mortality) under various emissions scenarios and used these predictions to estimate population dynamics. Fernandes et al. (2017) used the output of coupled hydrodynamics–biogeochemical models (including temperature and pH) under future emissions scenarios as inputs to a dynamic bio-climate envelope model (DBEM). OA effects were imposed on the growth of adults and the mortality rate of larvae. Their projected stock biomass and catch for multiple shellfish and demersal finfish species from present day to 2099 ranged from modest changes to positive effects for a few species (moderate emission scenarios) to major reductions in multiple species (mostly under the high emissions scenario). Queirós et al. (2015) used the same approach to simulate the changes in spatial distribution and abundance of dog whelk *Nucella lapillus*. A 60% decline in this mollusk was projected to occur by 2081–2100 relative to 1981–2000 abundances under a business-as-usual scenario (AR5 RCP8.5; IPCC 2014). Tai et al. (2018) also used life-history modeling and a sophisticated habitat-based DBEM approach to predict the changes in distribution and abundance of 10 NW Atlantic or NE Pacific marine invertebrate species. The modeling approach used Earth System Models to generate the inputs (temperature, CO_2, and primary production) as the basis for changing von-Bertalanffy growth curves and infer changes in life-history variables (mortality, maturity). The maximum projected change in abundances due to OA alone under emission scenarios (including RCP8.5) for 2091–2100 relative to 1996–2005 was 10%. Larger negative and positive responses across species were predicted when OA effects were combined with changes in temperature and primary production.

Two analyses illustrate how OA might affect S–R relationships. Koenigstein et al. (2018) developed a stage-oriented flow model that follows the number of individuals of Atlantic cod *Gadus morhua* from egg to 5 mo old juveniles (age-0) at a daily time step for a ~35 yr period (1983–2009) and then applied warmer temperatures and elevated CO_2. Their approach was similar to ours by simulating stages within the first year of life to predict recruitment and by imposing warming and OA effects as changes in mortality and duration of eggs, yolk-sac, and feeding larvae. The projected number of annual survivors of age-0 cod under the IPCC RCP8.5 scenario decreased by ~50% by 2100 with warming and OA. Stiasny et al. (2016) used an S–R approach and mortality based on elevated CO_2 from laboratory experiments for Western Baltic and Barents Sea cod stocks. They projected recruitment to decline by 8–24% by 2100 as pCO_2 increased from ~425–1100 µatm.

The Atlantis model has been used to simulate OA effects on complex food webs that depict ecosystems (Olsen et al. 2018). The general approach limited representation of OA effects to simple increases in mortality rates of the calcifying functional groups (e.g. corals, coccolithophores, echinoderms, and mollusks). The coordinated analysis reported by Olsen et al. (2018) uses versions of the model for 8 different regions and reported mostly small to moderate responses (one exception was large responses of Fay et al. 2017 at the functional group level). The magnitude of responses was further dampened when results were aggregated to the guild level.

Our study is the only one among the above-cited examples that used an individual-based modeling approach. There are a variety of reasons for following individuals rather than using habitat-based or Eulerian (e.g. population biomass) approaches (DeAngelis & Mooij 2005, DeAngelis & Grimm 2014).

Koenigstein et al. (2016) advocated for using an IBM approach for assessing OA effects because IBMs can be readily parameterized from experiments, can consider individual heterogeneity, and often facilitate a mechanistic understanding of how multiple factors (e.g. temperature and OA) interact. We opted for an IBM approach to capture the complicated exposures to temperature that interplay with elevated CO_2 effects imposed on specific processes and life stages. For example, the IBM approach naturally tracks the history of individuals, including how warming affects their development as embryos and yolk-sac larvae, and thereby determines their timing as larvae and juveniles. In terms of effects of elevated CO_2, altered growth rates of larvae are then superimposed on this warming effect and thus influence the timing of and the temperatures subsequently experienced by juveniles. Our use of super-individuals does reduce inter-individual variation and can be viewed numerically as a very detailed cohort model, with each super-individual acting as a cohort.

Our results from the Retrospective and Recovery simulations are largely comparable to the examples cited above that analyzed OA effects on fish. Consistent with our results, Fernandes et al. (2017) also found for their demersal fish species (sea bass, cod) that long-term biomass (2090–2099 vs. 1990–2000) was more affected by warming than the OA effect, and that OA responses were driven by OA effects on larvae. Under a high emissions scenario (warming and OA), they reported that the long-term biomass of both species was reduced by about 40%. This is in general agreement with our results for the Severe simulation that resulted in a 53.5% reduction in SSB over 40 yr. They also found evidence of the asymmetrical response that we documented; in their case, a positive OA effect on sea bass larvae was dampened (i.e. not manifested in biomass) by other processes in their model.

Our results were also similar in magnitude to the 2 analyses that examined OA effects directly on the S–R relationship. The prediction by Stiasny et al. (2016) that recruitment of cod would decrease to 8–25% of their reference levels is more dramatic than our predicted downward shift in the winter flounder S–R relationship (shown in Fig. 8). When our Severe simulation (combining several effects on early life stage mortality) was examined by decade (Table S3), we predicted average recruitment would be 22–50% of reference. Under warming and OA, Koenigstein et al. (2018) predicted recruitment to be 50% of their reference around 2050 (after about 30 yr), which was similar to our simulated recruitment with the Severe simulation (over 40 yr) being 34% of our reference. However, they found OA to have a larger effect than warming (20 vs. 35% of average recruitment by 2100). Using our Recovery experiment results (Table 10), we predicted warming (Reference conditions) would result in recruitment under Decade 4 conditions (warmest) that was 54% of the recruitment in Decade 1 (cool) conditions, while the Severe CO_2 effects generated a similar to smaller effect (50–76%, Severe/Reference for each decade). When Koenigstein et al. (2018) added adaptation, their predicted warming and OA effects were reduced, bringing their predicted responses more in alignment with our predictions.

When viewed from a high level, our methods and results can be considered consistent with the other modeling analyses that focused on fish. All relied on experimental results to specify the OA effects and typically imposed mortality and growth effects, often on early life stages. Each modeling analysis used different experimental results, involved different species, systems, and approaches, and used the environmental changes from different sources. Despite these differences, our short compilation of results suggests that for fish, warming has an important (if not dominant) role, implying that OA effects should be considered conditional on the temperature conditions. In addition, isolated OA effects (if multiple effects co-occur and are large individually) on recruitment and long-term population abundance are consistently predicted to be of ecologically important magnitude. However, the wide variety of ways OA effects were imposed in models shows there remain major knowledge gaps in how to translate OA effects measured in the laboratory into changes in growth and mortality processes of population and other modeling approaches.

4.4. Going forward

We view our modeling effort as a first step towards advancing the often-stated need for extrapolating laboratory effects of elevated CO_2 and OA effects to ecologically relevant scales. We have demonstrated how such population-level analyses, using laboratory results with individual-based modeling, could be done to provide quantitative projections of fish population dynamics under multiple stressors anticipated with climate change. Although our model included many uncertainties and assumptions that need empirical confirmation, and elevated CO_2 effects were imposed in a species-specific (winter flounder) model, our analysis provided a mechanistic view of how

warming and elevated CO_2 can interact and influence the long-term population dynamics of coastal fish species.

We advocate for more comparison and synthesis of the existing laboratory results so that a wide suite of effects can be represented with greater precision (Heuer & Grosell 2014, Pimentel et al. 2016, Cattano et al. 2018). This should be done in parallel with additional modeling (likely at the population to multispecies level) that enables direct comparisons of predictions across the different modeling analyses. A coordinated approach with different modeling groups using the same key environmental inputs from the same source, the same scenarios, and including analyses that isolate OA effects from other factors (e.g. temperature) would help in further determining likely OA effects at the population and higher levels. Determining why analyses generated similar or inconsistent results is difficult when many aspects of the models, imposed OA effects, and simulations (e.g. duration) differed. This was apparent with our cited examples, as well as within our analysis when a synergistic effect between warming and elevated CO_2 emerged with the Recovery experiment but was not detected in the Retrospective experiment. We agree with Tai et al. (2018) that the formulation of OA effects and climate change scenarios remain as major contributors to uncertainties in modeling OA effects on fish and shellfish populations.

Acknowledgements. This study was funded by a NOAA Ocean Acidification Program Data Synthesis award to R.C.C., K.A.R., and K.B.H. K.B.H. was funded through the Cooperative Institute for the North Atlantic Region (CINAR) under Cooperative Agreement NA14OAR4320158. The anonymous reviewers offered many insightful comments leading to improvements in the manuscript. This is UMCES contribution No. 5953.

LITERATURE CITED

Able KW, Grothues TM, Morson JM, Coleman KE (2014) Temporal variation in winter flounder recruitment at the southern margin of their range: Is the decline due to increasing temperatures? ICES J Mar Sci 71:2186–2197

Andersson AJ, Kline DI, Edmunds PJ, Archer SD and others (2015) Understanding ocean acidification impacts on organismal to ecological scales. Oceanography (Wash DC) 28:16–27

Archambault B, Rivot E, Savina M, Le Pape O (2018) Using a spatially structured life cycle model to assess the influence of multiple stressors on an exploited coastal-nursery-dependent population. Estuar Coast Shelf Sci 201: 95–104

Bartley TJ, McCann KS, Bieg C, Cazelles K and others (2019) Food web rewiring in a changing world. Nat Ecol Evol 3:345–354

Baumann H (2019) Experimental assessments of marine species sensitivities to ocean acidification and co-stressors: How far have we come? Can J Zool 97:399–408

Baumann H, Talmage SC, Gobler CJ (2012) Reduced early life growth and survival in a fish in direct response to increased carbon dioxide. Nat Clim Chang 2:38–41

Baumann H, Wallace RB, Tagliaferri T, Gobler CJ (2015) Large natural pH, CO_2 and O_2 fluctuations in a temperate tidal salt marsh on diel, seasonal, and interannual time scales. Estuaries Coasts 38:220–231

Bell RJ, Hare JA, Manderson JP, Richardson DE (2014) Externally driven changes in the abundance of summer and winter flounder. ICES J Mar Sci 71:2416–2428

Bivand R, Lewin-Koh N (2021) maptools: tools for handling spatial objects. R package version 1.1-2. https://CRAN.R-project.org/package=maptools

Buckley LJ (1981) Biochemical changes during ontogenesis of cod (*Gadus morhua* L.) and winter flounder (*Pseudopleuronectes americanus*) larvae. Rapp P-V Réun Cons Int Éxplor Mer 178:547–552

Buckley LJ, Smigielski AS, Halavik TA, Laurence GC (1990) Effects of water temperature on size and biochemical composition of winter flounder *Pseudopleuronectes americanus* at hatching and feeding initiation. Fish Bull 88:419–428

Buckley LJ, Smigielski AS, Halavik TA, Caldarone EM, Burns BR, Laurence GC (1991) Winter flounder *Pseudopleuronectes americanus* reproductive success. II. Effects of spawning time and female size on size, composition and viability of eggs and larvae. Mar Ecol Prog Ser 74:125–135

Cattano C, Claudet J, Domenici P, Milazzo M (2018) Living in a high CO_2 world: a global meta-analysis shows multiple trait-mediated fish responses to ocean acidification. Ecol Monogr 88:320–335

Cetta CM, Capuzzo JM (1982) Physiological and biochemical aspects of embryonic and larval development of the winter flounder *Pseudopleuronectes americanus*. Mar Biol 71:327–337

Chambers RC, Rose KA, Tyler JA (1995) Recruitment and recruitment processes of winter flounder, *Pleuronectes americanus*, at different latitudes, implications of an individual-based simulation model. Neth J Sea Res 34: 19–43

Chambers RC, Candelmo AC, Habeck EA, Poach ME and others (2014) Effects of elevated CO_2 in the early life stages of summer flounder, *Paralichthys dentatus*, and potential consequences of ocean acidification. Biogeosciences 11:1613–1626

Clements JC, Hunt HL (2015) Marine animal behaviour in a high CO_2 ocean. Mar Ecol Prog Ser 536:259–279

Conn PB, Williams EH, Shertzer KW (2010) When can we reliably estimate the productivity of fish stocks? Can J Fish Aquat Sci 67:511–523

Danila DJ (2000) Estimating the abundance and egg production of spawning winter flounder (*Pseudopleuronectes americanus*) in the Niantic River, CT for use in the assessment of impact at Millstone Nuclear Power Station. Environ Sci Policy 3:459–469

DeAngelis DL, Grimm V (2014) Individual-based models in ecology after four decades. F1000Prime Rep 6:39

DeAngelis DL, Mooij WM (2005) Individual-based modeling of ecological and evolutionary processes. Annu Rev Ecol Evol Syst 36:147–168

DeLong AK, Collie JS, Meise CJ, Powell JC (2001) Estimating growth and mortality of juvenile winter flounder, *Pseudopleuronectes americanus*, with a length-based model. Can J Fish Aquat Sci 58:2233–2246

DePasquale E, Baumann H, Gobler CJ (2015) Vulnerability of early life stage Northwest Atlantic forage fish to ocean acidification and low oxygen. Mar Ecol Prog Ser 523: 145–156

Deslauriers D, Chipps SR, Breck JE, Rice JA, Madenjian CP (2017) Fish bioenergetics 4.0: an R-based modeling application. Fisheries (Bethesda, Md) 42:586–596

Fay G, Link JS, Hare JA (2017) Assessing the effects of ocean acidification in the Northeast US using an end-to-end marine ecosystem model. Ecol Modell 347:1–10

Fernandes JA, Papathanasopoulou E, Hattam C, Queirós AM and others (2017) Estimating the ecological, economic and social impacts of ocean acidification and warming on UK fisheries. Fish Fish 18:389–411

Frame DW (1973a) Biology of young winter flounder *Pseudopleuronectes americanus* (Walbaum); metabolism under simulated estuarine conditions. Trans Am Fish Soc 102:423–430

Frame DW (1973b) Conversion efficiency and survival of young winter flounder (*Pseudopleuronectes americanus*) under experimental conditions. Trans Am Fish Soc 102: 614–617

Frommel AY, Maneja R, Lowe D, Malzahn AM and others (2012) Severe tissue damage in Atlantic cod larvae under increasing ocean acidification. Nat Clim Chang 2:42–46

Gargett AE, Li M, Brown R (2001) Testing mechanistic explanations of observed correlations between environmental factors and marine fisheries. Can J Fish Aquat Sci 58:208–219

Gaylord B, Kroeker KJ, Sunday JM, Anderson KM and others (2015) Ocean acidification through the lens of ecological theory. Ecology 96:3–15

Gobler CJ, Merlo LR, Morrell BK, Griffith AW (2018) Temperature, acidification, and food supply interact to negatively affect the growth and survival of the forage fish, *Menidia beryllina* (inland silverside), and *Cyprinodon variegatus* (sheepshead minnow). Front Mar Sci 5:86

Gräns A, Jutfelt F, Sandblom E, Jönsson E and others (2014) Aerobic scope fails to explain the detrimental effects on growth resulting from warming and elevated CO_2 in Atlantic halibut. J Exp Biol 217:711–717

Hare JA, Morrison WE, Nelson MW, Stachura MM and others (2016) A vulnerability assessment of fish and invertebrates to climate change on the Northeast US continental shelf. PLOS ONE 11:e0146756

Hartin CA, Bond-Lamberty B, Patel P, Mundra A (2016) Ocean acidification over the next three centuries using a simple global climate carbon-cycle model: projections and sensitivities. Biogeosciences 13:4329–4342

Harvey BP, Gwynn-Jones D, Moore PJ (2013) Meta-analysis reveals complex marine biological responses to the interactive effects of ocean acidification and warming. Ecol Evol 3:1016–1030

Heuer RM, Grosell M (2014) Physiological impacts of elevated carbon dioxide and ocean acidification on fish. Am J Physiol Regul Integr Comp Physiol 307:R1061–R1084

Hofmann GE, Barry JP, Edmunds PJ, Gates RD, Hutchins DA, Klinger T, Sewell MA (2010) The effect of ocean acidification on calcifying organisms in marine ecosystems: an organism-to-ecosystem perspective. Annu Rev Ecol Evol Syst 41:127–147

Houde ED, Zastrow CE (1993) Ecosystem-and taxon-specific dynamic and energetics properties of larval fish assemblages. Bull Mar Sci 53:290–335

Huebert KB, Peck MA (2014) A day in the life of fish larvae: modeling foraging and growth using Quirks. PLOS ONE 9:e98205

Huebner JD, Langton RW (1982) Rate of gastric evacuation for winter flounder, *Pseudopleuronectes americanus*. Can J Fish Aquat Sci 39:356–360

Hurst TP, Fernandez ER, Mathis JT (2013) Effects of ocean acidification on hatch size and larval growth of walleye pollock (*Theragra chalcogramma*). ICES J Mar Sci 70: 812–822

Hurst TP, Laurel BJ, Mathis JT, Tobosa LR (2016) Effects of elevated CO_2 levels on eggs and larvae of a North Pacific flatfish. ICES J Mar Sci 73:981–990

IPCC (2014) Climate change 2014: synthesis report. Contribution of Working Groups I, II and III to the Fifth Assessment Report of the Intergovernmental Panel on Climate Change. IPCC, Geneva

Jeffries HP, Terceiro M (1985) Cycle of changing abundances in the fishes of the Narragansett Bay area. Mar Ecol Prog Ser 25:239–244

Keller AA, Klein-MacPhee G (2000) Impact of elevated temperature on the growth, survival, and trophic dynamics of winter flounder larvae: a mesocosm study. Can J Fish Aquat Sci 57:2382–2392

Kim KS, Shim JH, Kim S (2015) Effects of CO_2-induced ocean acidification on the growth of the larval olive flounder *Paralichthys olivaceus*. Ocean Sci J 50:381–388

Klein-MacPhee G (1978) Synopsis of biological data for the winter flounder *Pseudopleuronectes americans* (Walbaum). NOAA Tech Rep NMFS CIRC 414

Koenigstein S, Mark FC, Gößling-Reisemann S, Reuter H, Poertner HO (2016) Modelling climate change impacts on marine fish populations: process-based integration of ocean warming, acidification and other environmental drivers. Fish Fish 17:972–1004

Koenigstein S, Dahlke FT, Stiasny MH, Storch D, Clemmesen C, Pörtner HO (2018) Forecasting future recruitment success for Atlantic cod in the warming and acidifying Barents Sea. Glob Change Biol 24:526–535

Laurence GC (1975) Laboratory growth and metabolism of the winter flounder *Pseudopleuronectes americanus* from hatching through metamorphosis at three temperatures. Mar Biol 32:223–229

Laurence GC (1977) A bioenergetic model for the analysis of feeding and survival potential of winter flounder, *Pseudopleuronectes americanus*, larvae during the period from hatching to metamorphosis. Fish Bull 75:529–546

Le Quesne WJF, Pinnegar JK (2012) The potential impacts of ocean acidification: scaling from physiology to fisheries. Fish Fish 13:333–344

Lorda E, Danila DJ, Miller JD (2000) Application of a population dynamics model to the probabilistic assessment of cooling water intake effects of Millstone Nuclear Power Station (Waterford, CT) on a nearby winter flounder spawning stock. Environ Sci Policy 3(Suppl 1):471–482

Lorenzen K, Enberg K (2002) Density-dependent growth as a key mechanism in the regulation of fish populations: evidence from among-population comparisons. Proc R Soc B 269:49–54

Machado M, Arenas F, Svendsen JC, Azeredo R, Pfeifer LJ, Wilson JM, Costas B (2020) Effects of water acidification on Senegalese sole *Solea senegalensis* health status and

metabolic rate: implications for immune responses and energy use. Front Physiol 11:26
Manderson JP, Phelan BA, Meise C, Stehlik LL and others (2002) Spatial dynamics of habitat suitability for the growth of newly settled winter flounder *Pseudopleuronectes americanus* in an estuarine nursery. Mar Ecol Prog Ser 228:227–239
Mangel M, Brodziak J, DiNardo G (2010) Reproductive ecology and scientific inference of steepness: a fundamental metric of population dynamics and strategic fisheries management. Fish Fish 11:89–104
McBride RS, Wuenschel MJ, Nitschke P, Thornton G, King JR (2013) Latitudinal and stock-specific variation in size- and age-at-maturity of female winter flounder, *Pseudopleuronectes americanus*, as determined with gonad histology. J Sea Res 75:41–51
McElroy WD, Wuenschel MJ, Press YK, Towle EK, McBride RS (2013) Differences in female individual reproductive potential among three stocks of winter flounder, *Pseudopleuronectes americanus*. J Sea Res 75:52–61
Meng L, Gray C, Taplin B, Kupcha E (2000) Using winter flounder growth rates to assess habitat quality in Rhode Island's coastal lagoons. Mar Ecol Prog Ser 201:287–299
Midway SR, White JW, Scharf FS (2018) The potential for cryptic population structure to sustain a heavily exploited marine flatfish stock. Mar Coast Fish 10:411–423
Millstone Environmental Laboratory (2017) Winter flounder studies. In: Dominion Nuclear Connecticut, Inc. Annual report 2016. Monitoring the marine environment of Long Island Sound at Millstone Power Station, Waterford, Connecticut. Millstone Environmental Laboratory, Waterford, CT, p 111–144
Morrongiello JR, Walsh CT, Gray CA, Stocks JR, Crook DA (2014) Environmental change drives long-term recruitment and growth variation in an estuarine fish. Glob Change Biol 20:1844–1860
Munday PL, Crawley NE, Nilsson GE (2009) Interacting effects of elevated temperature and ocean acidification on the aerobic performance of coral reef fishes. Mar Ecol Prog Ser 388:235–242
Munday PL, Dixson DL, McCormick MI, Meekan M, Ferrari MCO, Chivers DP (2010) Replenishment of fish populations is threatened by ocean acidification. Proc Natl Acad Sci USA 107:12930–12934
Myers RA (1998) When do environment–recruitment correlations work? Rev Fish Biol Fish 8:285–305
Myers RA, Cadigan NG (1993) Density-dependent juvenile mortality in marine demersal fish. Can J Fish Aquat Sci 50:1576–1590
Nagelkerken I, Munday PL (2016) Animal behaviour shapes the ecological effects of ocean acidification and warming: moving from individual to community-level responses. Glob Change Biol 22:974–989
NEFSC (Northeast Fisheries Science Center) (2011) 52nd Northeast regional stock assessment workshop (52nd SAW) assessment summary report. NEFSC Ref Doc 11-11. Northeast Fisheries Science Center, Woods Hole, MA
Nye JA, Link JS, Hare JA, Overholtz WJ (2009) Changing spatial distribution of fish stocks in relation to climate and population size on the Northeast United States continental shelf. Mar Ecol Prog Ser 393:111–129
Olsen E, Kaplan IC, Ainsworth C, Fay G and others (2018) Ocean futures under ocean acidification, marine protection, and changing fishing pressures explored using a worldwide suite of ecosystem models. Front Mar Sci 5:64
Ottersen G, Kim S, Huse G, Polovina JJ, Stenseth NC (2010) Major pathways by which climate may force marine fish populations. J Mar Syst 79:343–360
Pankhurst NW, Munday PL (2011) Effects of climate change on fish reproduction and early life history stages. Mar Freshw Res 62:1015–1026
Pasquaud S, Courrat A, Fonseca VF, Gamito R and others (2013) Strength and time lag of relationships between human pressures and fish-based metrics used to assess ecological quality of estuarine systems. Estuar Coast Shelf Sci 134:119–127
Pearcy WG (1962) Ecology of an estuarine population of winter flounder, *Pseudopleuronectes americanus* (Walbaum). Parts I–IV. Bull Bingham Oceanogr Collect 18(1): 1–77
Pereira J, Goldberg R, Ziskowski J, Berrien P, Morse W, Johnson D (1999) Essential fish habitat source document: winter flounder, *Pseudopleuronectes americanus*, life history and habitat characteristics. NOAA Tech Memo NMFS-NE-138
Petitgas P, Rijnsdorp AD, Dickey-Collas M, Engelhard GH and others (2013) Impacts of climate change on the complex life cycles of fish. Fish Oceanogr 22:121–139
Pimentel MS, Faleiro F, Machado J, Rosa R (2015) Compromised development of flatfish (*Solea senegalensis*) larvae under ocean warming and acidification. Microsc Microanal 21:16–17
Pimentel MS, Faleiro F, Marques T, Bispo R and others (2016) Foraging behaviour, swimming performance and malformations of early stages of commercially important fishes under ocean acidification and warming. Clim Change 137:495–509
Potter IC, Tweedley JR, Elliott M, Whitfield AK (2015) The ways in which fish use estuaries: a refinement and expansion of the guild approach. Fish Fish 16:230–239
Queirós AM, Fernandes JA, Faulwetter S, Nunes J and others (2015) Scaling up experimental ocean acidification and warming research: from individuals to the ecosystem. Glob Change Biol 21:130–143
R Development Core Team (2016) R: a language and environment for statistical computing. R Foundation for Statistical Computing, Vienna
Rijnsdorp AD (1994) Population-regulating processes during the adult phase in flatfish. Neth J Sea Res 32:207–223
Rogers CA (1976) Effects of temperature and salinity on the survival of winter flounder embryos. Fish Bull 74:52–58
Rogers LA, Dougherty AB (2019) Effects of climate and demography on reproductive phenology of a harvested marine fish population. Glob Change Biol 25:708–720
Rose KA (2000) Why are quantitative relationships between environmental quality and fish populations so elusive? Ecol Appl 10:367–385
Rose KA, Tyler JA, Chambers RC, Klein-MacPhee G, Danila DJ (1996) Simulating winter flounder population dynamics using coupled individual-based young-of-the-year and age-structured adult models. Can J Fish Aquat Sci 53:1071–1091
Rose KA, Cowan JH, Winemiller KO, Myers RA, Hilborn R (2001) Compensatory density dependence in fish populations: importance, controversy, understanding and prognosis: compensation in fish populations. Fish Fish 2: 293–327
Rose KA, Murphy CA, Diamond SL, Fuiman LA, Thomas P (2003) Using nested models and laboratory data for predicting population effects of contaminants on fish: a step

toward a bottom-up approach for establishing causality in field studies. Hum Ecol Risk Assess 9:231–257

Rose KA, Fiechter J, Curchitser EN, Hedstrom K and others (2015) Demonstration of a fully-coupled end-to-end model for small pelagic fish using sardine and anchovy in the California Current. Prog Oceanogr 138:348–380

Scheffer M, Baveco JM, DeAngelis DL, Rose KA, van Nes EH (1995) Super-individuals a simple solution for modelling large populations on an individual basis. Ecol Modell 80:161–170

Shertzer KW, Conn PB (2012) Spawner–recruit relationships of demersal marine fishes: prior distribution of steepness. Bull Mar Sci 88:39–50

Sogard SM (1992) Variability in growth rates of juvenile fishes in different estuarine habitats. Mar Ecol Prog Ser 85:35–53

Sswat M, Stiasny MH, Jutfelt F, Riebesell U, Clemmesen C (2018) Growth performance and survival of larval Atlantic herring, under the combined effects of elevated temperatures and CO_2. PLOS ONE 13:e0191947

Stiasny MH, Mittermayer FH, Sswat M, Voss R and others (2016) Ocean acidification effects on Atlantic cod larval survival and recruitment to the fished population. PLOS ONE 11:e0155448

Stiasny MH, Mittermayer FH, Göttler G, Bridges CR and others (2018) Effects of parental acclimation and energy limitation in response to high CO_2 exposure in Atlantic cod. Sci Rep 8:8348

Stiasny MH, Sswat M, Mittermayer FH, Falk-Petersen IB and others (2019) Divergent responses of Atlantic cod to ocean acidification and food limitation. Glob Change Biol 25:839–849

Suter GW II (2016) Ecological risk assessment. CRC Press, Boca Raton, FL

Tai TC, Harley CDG, Cheung WWL (2018) Comparing model parameterizations of the biophysical impacts of ocean acidification to identify limitations and uncertainties. Ecol Modell 385:1–11

Taylor DL (2005) Predation on post-settlement winter flounder *Pseudopleuronectes americanus* by sand shrimp *Crangon septemspinosa* in NW Atlantic estuaries. Mar Ecol Prog Ser 289:245–262

Thornton KW, Lessem AS (1978) A temperature algorithm for modifying biological rates. Trans Am Fish Soc 107: 284–287

Townsend H, Harvey CJ, deReynier Y, Davis D and others (2019) Progress on implementing ecosystem-based fisheries management in the United States through the use of ecosystem models and analysis. Front Mar Sci 6:641

Tyler JA, Rose KA, Chambers RC (1997) Compensatory responses to decreased young-of-the-year survival: an individual-based modelling analysis of winter flounder. In: Chambers RC, Trippel EA (eds) Early life history and recruitment in fish populations. Fish and Fisheries Series, Vol 21. Chapman & Hall, London, p 391–422

van der Veer HW, Berghahn R, Miller JM, Rijnsdorp AD (2000) Recruitment in flatfish, with special emphasis on North Atlantic species: progress made by the Flatfish Symposia. ICES J Mar Sci 57:202–215

Voyer RA, Morrison GE (1971) Factors affecting respiration rates of winter flounder (*Pseudopleuronectes americanus*). J Fish Res Board Can 28:1907–1911

Watson SA, Allan BJM, McQueen DE, Nicol S and others (2018) Ocean warming has a greater effect than acidification on the early life history development and swimming performance of a large circumglobal pelagic fish. Glob Change Biol 24:4368–4385

Williams GC (1975) Viable embryogenesis of the winter flounder *Pseudopleuronectes americanus* from −1.8° to 15°C. Mar Biol 33:71–74

Witherell DB, Burnett J (1993) Growth and maturation of winter flounder, *Pleuronectes americanus*, in Massachusetts. Fish Bull 91:816–820

Worobec MN (1984) Field estimates of the daily ration of winter flounder, *Pseudopleuronectes americanus* (Walbaum), in a southern New England salt pond. J Exp Mar Biol Ecol 77:183–196

Ziegler CM, Zacharias JP, Frisk MG (2018) Migration diversity, spawning behavior, and habitat utilization of winter flounder. Can J Fish Aquat Sci 76:1503–1514

Editorial responsibility: Alejandro Gallego, Aberdeen, UK
Reviewed by: 3 anonymous referees

Submitted: February 5, 2021
Accepted: September 16, 2021
Proofs received from author(s): November 16, 2021